Mechanisms Preserving Insulin Action during High Dietary Fat Intake

Article *in* Cell Metabolism · September 2018

DOI: 10.1016/j.cmet.2018.08.022

CITATION
1

READS
130

19 authors, including:

Annemarie Lundsgaard
University of Copenhagen
15 PUBLICATIONS **158** CITATIONS
SEE PROFILE

Jacob Bak Holm
Clinical Microbiomics
21 PUBLICATIONS **558** CITATIONS
SEE PROFILE

Kim Sjøberg
University of Copenhagen
28 PUBLICATIONS **290** CITATIONS
SEE PROFILE

Lene Secher Myrmel
Institute of Marine Research in Norway
18 PUBLICATIONS **117** CITATIONS
SEE PROFILE

Clinical and Translational Report

Cell Metabolism

Mechanisms Preserving Insulin Action during High Dietary Fat Intake

Graphical Abstract

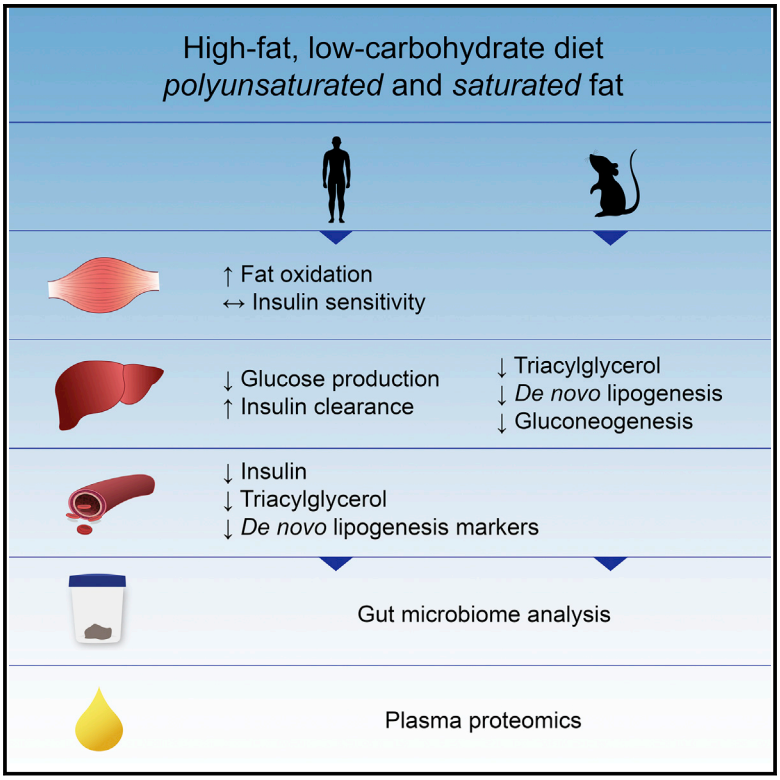

Highlights

- Insulin sensitivity is maintained in both men and mice with high PUFA or SFA intake
- Hepatic glucose production and *de novo* lipogenesis are decreased with high fat intake
- High fat intake decreases fasting insulin and triacylglycerol levels
- High fat intake changes the plasma proteome in an immune-supporting direction

Authors

Anne-Marie Lundsgaard, Jacob B. Holm, Kim A. Sjøberg, ..., Jørgen F.P. Wojtaszewski, Erik A. Richter, Bente Kiens

Correspondence

bkiens@nexs.ku.dk

In Brief

Lundsgaard et al. reveal the adaptations in muscle, liver, blood, and gut that maintain peripheral insulin sensitivity, lower circulating lipids, and decrease hepatic *de novo* lipogenesis and gluconeogenesis when humans and mice ingest a high-fat diet for 6 weeks enriched in either polyunsaturated or saturated fatty acids.

Lundsgaard et al., 2019, Cell Metabolism *29*, 1–14
January 8, 2019
https://doi.org/10.1016/j.cmet.2018.08.022

CellPress

Please cite this article in press as: Lundsgaard et al., Mechanisms Preserving Insulin Action during High Dietary Fat Intake, Cell Metabolism (2018), https://doi.org/10.1016/j.cmet.2018.08.022

Cell Metabolism
Clinical and Translational Report

Mechanisms Preserving Insulin Action during High Dietary Fat Intake

Anne-Marie Lundsgaard,[1] Jacob B. Holm,[2,6] Kim A. Sjøberg,[1] Kirstine N. Bojsen-Møller,[3] Lene S. Myrmel,[4] Even Fjære,[4] Benjamin A.H. Jensen,[2,7] Trine S. Nicolaisen,[1] Janne R. Hingst,[1] Sine L. Hansen,[1] Sophia Doll,[8] Philip E. Geyer,[8] Atul S. Deshmukh,[9] Jens J. Holst,[5] Lise Madsen,[2,4] Karsten Kristiansen,[2,10] Jørgen F.P. Wojtaszewski,[1] Erik A. Richter,[1] and Bente Kiens[1,11,*]

[1]Section of Molecular Physiology, Department of Nutrition, Exercise and Sports, Faculty of Science, University of Copenhagen, Universitetsparken 13, Copenhagen 2100, Denmark
[2]Laboratory of Genomics and Molecular Biomedicine, Department of Biology, University of Copenhagen, Copenhagen, Denmark
[3]Department of Endocrinology, Hvidovre University Hospital, Hvidovre, Denmark
[4]Institute of Marine Research, Bergen, Norway
[5]Novo Nordisk Foundation Center for Basic Metabolic Research and Department of Biomedical Sciences, Faculty of Health and Medical Sciences, University of Copenhagen, Copenhagen, Denmark
[6]Clinical Microbiomics, Copenhagen, Denmark
[7]Department of Medicine, Laval University, Quebec, QC, Canada
[8]Department of Proteomics and Signal Transduction, Max-Planck-Institute of Biochemistry, Munich, Germany
[9]The Novo Nordisk Foundation Center for Protein Research, Clinical Proteomics, Faculty of Health and Medical Sciences, University of Copenhagen, Copenhagen, Denmark
[10]Institute of Metagenomics, BGI-Shenzhen, Shenzhen, China
[11]Lead Contact
*Correspondence: bkiens@nexs.ku.dk
https://doi.org/10.1016/j.cmet.2018.08.022

SUMMARY

Prolonged intervention studies investigating molecular metabolism are necessary for a deeper understanding of dietary effects on health. Here we provide mechanistic information about metabolic adaptation to fat-rich diets. Healthy, slightly overweight men ingested saturated or polyunsaturated fat-rich diets for 6 weeks during weight maintenance. Hyperinsulinemic clamps combined with leg balance technique revealed unchanged peripheral insulin sensitivity, independent of fatty acid type. Both diets increased fat oxidation potential in muscle. Hepatic insulin clearance increased, while glucose production, *de novo* lipogenesis, and plasma triacylglycerol decreased. High fat intake changed the plasma proteome in the immune-supporting direction and the gut microbiome displayed changes at taxonomical and functional level with polyunsaturated fatty acid (PUFA). In mice, eucaloric feeding of human PUFA and saturated fatty acid diets lowered hepatic triacylglycerol content compared with low-fat-fed control mice, and induced adaptations in the liver supportive of decreased gluconeogenesis and lipogenesis. Intake of fat-rich diets thus induces extensive metabolic adaptations enabling disposition of dietary fat without metabolic complications.

INTRODUCTION

Dietary guidelines have for decades advocated to limit the dietary intake of total fat in order to preserve overall health. At the same time, the level of available evidence on total fat intake and the associated risk of diabetes and metabolic syndrome components is still considered insufficient (FAO, 2010). Recent cohort studies have actually shown that increased dietary fat intake reduced mortality and was not linked to cardiovascular disease (Dehghan et al., 2017) or type 2 diabetes incidence (Schwab et al., 2014), and that intake of dietary saturated fatty acids (SFAs), which has long been perceived as unhealthy, was not associated with increased risk of insulin resistance or cardiovascular disease (Astrup, 2014; Morio et al., 2016; Aune et al., 2013).

The use of large epidemiological cohort studies is, however, not expedient for identification of the optimal diet due to inherent difficulty of getting mechanistic insight into molecular metabolism of dietary components. Indeed, many intervention studies have reported reduced insulin sensitivity following high fatty acid (FA) exposure to different cell types in culture, ad libitum high-fat feeding in rodents, and acute intravenous triacylglycerol (TG) and heparin administration, elevating plasma FA concentrations 5- to 6-fold compared with resting post-absorptive levels, in healthy humans (Pehmoller et al., 2012; Hoeg et al., 2011; Gormsen et al., 2007). However, when lipids are provided in a more physiologic context by ingestion of a fat-rich diet, intervention studies of up to 3 weeks' duration have indicated that the ability of insulin to stimulate glucose disposal is not impaired in healthy lean or overweight subjects after intake of weight-maintaining diets with a total fat content of 49E%–83E% (percentage

of total energy intake) (Cutler et al., 1995; Bisschop et al., 2001; Skovbro et al., 2011; Yost et al., 1998; van Herpen et al., 2011; Borkman et al., 1991). This is despite the fact that the daily fat intake comprised up to 3-fold the amount administered in lipid infusion studies. Thus, solid mechanistic intervention studies in humans investigating how the human organism handles dietary FAs at the molecular level are clearly warranted.

The purpose of the present study was, therefore, to investigate insulin sensitivity, substrate metabolism, and molecular mechanisms accompanying prolonged increased exposure to dietary FAs, at the level of skeletal muscle and the liver, key organs regulating whole-body metabolism. The hyperinsulinemic-euglycemic clamp was combined with glucose tracer infusion for determination of hepatic glucose production, skeletal muscle biopsies, and the femoral arteriovenous (a-v) balance technique, enabling assessment of insulin sensitivity directly at the level of skeletal muscle, the main site of insulin-stimulated glucose disposal (Orava et al., 2013). Two experimental high-fat diets, equally rich in total fat but varying markedly in content of SFAs and polyunsaturated FAs (PUFAs), were designed to assess whether the adaptive mechanisms are FA-type specific. The study involved slightly overweight and untrained subjects, a typical population group prone to develop metabolic diseases. The intervention length was 6 weeks, with energy provision set to match eucaloric requirements of the volunteers and keep their body weights stable.

To gain insight into liver-specific molecular adaptations to high fat intake, mice fed with the same saturated and polyunsaturated high-fat diets for 6 weeks were also investigated. To match the eucaloric human design, both high-fat diets were provided in a pair-feeding manner based on the energy intake of mice fed a low-fat control diet. Thereby, the effect of increased fat intake per se, independent of potential diet-induced obesity, could be studied. Feces samples from both humans and mice were obtained to investigate the adaptation in gut microbiome composition and its functional potential, and the plasma proteome was investigated to give a global view of the integrated metabolic response.

RESULTS AND DISCUSSION

Eighteen healthy, young (33 ± 6 years), overweight (BMI 26.4 ± 2.4 kg m^{-2}), and untrained (peak oxygen uptake [VO_2peak] 39.1 ± 5.2 mL kg^{-1} min^{-1}) men were included in the study, and by a parallel intervention design randomized to 6 weeks on a high-fat diet enriched in either PUFA (n = 9) or SFAs (n = 9) (Figure S1). Both diets comprised 64E% fat, 16E% protein, and 20E% carbohydrate, resulting in an increase in fat intake by 30E% and carbohydrate intake decrease by 26E% compared with their habitual intake (Table S1). The intervention was conducted in a highly controlled and daily supervised free-living setting. All foods and drinks were delivered to the subjects, after being weighed and pre-packed. It was supervised that subjects did not change their physical activity levels. Consistent with the design, body weight remained stable during both interventions, with no change in body composition (Table 1). The metabolism of the subjects was then investigated before and after 6 weeks of intervention.

Six weeks' eucaloric intake of the 64E% high-fat diets did not compromise insulin's ability to stimulate whole-body glucose disposal compared with pre intervention (Figure 1A), when assessed by the hyperinsulinemic-euglycemic clamp (1 mU insulin kg^{-1} min^{-1}). These findings were obtained when 34E% of the dietary fat was polyunsaturated, comprising in particular C18:2n-6 and C18:3n-3 FAs from vegetable oils, fatty fish, nuts, and seeds, but also when 39E% was saturated fat, in particular C16:0 and C18:0 from high-fat dairy and fatty meat (Table S1; Figure S1).

Thus, irrespective of FA type, when caloric intake is balanced, insulin sensitivity was maintained. The insulin/glucose homeostasis in the fasting state was actually changed in a non-diabetic direction, as fasting plasma insulin concentration decreased after both high-fat diets (Table 1). Additionally, fasting plasma TG concentrations were markedly reduced after both high-fat diets (Table 1), which would be beneficial in terms of dyslipidemia and cardiovascular risk. The plasma cholesterol profile remained unchanged after the SFA diet, and was changed in a beneficial direction after PUFA intake, as total cholesterol decreased and low-density lipoprotein-cholesterol tended to decrease, while high-density lipoprotein-cholesterol was unchanged (Table 1).

Together, these findings raise questions regarding the mechanisms enabling the organism to handle increased lipid availability without metabolic deterioration.

Increased Contribution of Fat to Energy Utilization

A major metabolic shift occurs when a diet high in fat and low in carbohydrates is consumed. In the overnight-fasted, resting state, the basal metabolic rate remained unchanged while respiratory exchange ratio (RER) values decreased markedly after both high-fat diets, indicating an increased contribution of FA combustion to energy utilization (Figures 1B and 1C). Skeletal muscle represents a major site of energy utilization. Accordingly, when challenged with increased dietary FA availability, the protein content of the lipid transporter cluster of differentiation 36/SR-B2 (CD36) in muscle biopsies increased similarly after both high-fat diets (Figure 1D), permitting an increased trans-membrane uptake of plasma FAs. The upregulation of CD36 protein was complemented by an increased capacity for intracellular FA handling, as the protein content of fatty acid transport protein 1 (FATP1) and 4 (FATP4) in muscle also increased after the two diets (Figures 1E and 1F). Irrespective of PUFA or SFA diet, post-intervention high-fat (75E%) meal tests (Table S2) showed markedly lower postprandial plasma TG concentrations (42% and 45% lower area under the curve compared with pre intervention) (Figures 1G and 1H). Concomitantly, the 5 hr postprandial FA oxidation was higher and accounted for almost 100% of energy utilization post intervention (Figure 1I).

Pyruvate dehydrogenase E1α (PDH-E1α) plays a key role controlling the balance between glucose and FA oxidation. The increased FA oxidation was observed concomitantly with increased phosphorylation of basal muscle PDH-E1α at the Ser^{300} site after both PUFA and SFA, and Ser^{293} after SFA (Figures 1J–1L), indicating covalent PDH inactivation and decreased pyruvate conversion to acetyl coenzyme A (CoA), enabling greater uptake of beta-oxidation-derived acetyl-CoA into the TCA cycle. An allosteric inhibition of PDH activity by increased acetyl-CoA and NADH content, or lower pyruvate, could potentially also have contributed. Thus, when rat heart mitochondria were exposed to increased FA availability, acetyl-CoA levels increased and allosterically inactivated PDH (Kerbey et al.,

Table 1. Body Composition and Arterialized Plasma Parameters

	PUFA		SFA				
	Pre	Post	Pre	Post	Intervention	Diet	Intervention × Diet
Body Composition							
Body weight (kg)	87.5 ± 1.9	86.2 ± 2.4	91.9 ± 2.6	92.0 ± 2.4			
Lean body mass (kg)	60.8 ± 1.4	60.2 ± 1.6	62.3 ± 1.9	62.4 ± 1.8			
Fat mass (kg)	23.2 ± 1.4	22.6 ± 1.6	26.1 ± 1.7	26.0 ± 1.9			
Visceral fat (g)	820 ± 164	758 ± 146	797 ± 95	770 ± 132			
Plasma Parameters							
Glucose (mmol L^{-1})	5.6 ± 0.1	5.4 ± 0.1	5.6 ± 0.1	5.5 ± 0.2			
Insulin (μU mL^{-1})	4.6 ± 0.9	3.5 ± 0.5	4.7 ± 1.2	2.7 ± 0.7	**		
C peptide (pmol L^{-1})	434 ± 108	399 ± 70	479 ± 68	410 ± 60			
HOMA-IR index	1.2 ± 0.2	0.8 ± 0.1	1.1 ± 0.3	0.7 ± 0.2	**		
Glucagon (pmol L^{-1})	6.7 ± 0.5	9.5 ± 1.0^^^	6.4 ± 0.6	6.4 ± 0.7			**
Insulin clearance (mL·min^{-1})	14.3 ± 3.2	20.4 ± 7.2	16.9 ± 2.9	36.3 ± 11.4	**		
hsCRP mg L^{-1}	0.91 ± 0.29	0.40 ± 0.15	0.68 ± 0.15	0.62 ± 0.22	p = 0.076		
ALAT (U L^{-1})	35.9 ± 4.0	37.3 ± 2.6	37.6 ± 2.4	39.8 ± 3.2			
3-Hydroxybutyrate (μmol·L^{-1})	67.8 ± 25.6	297.8 ± 67.4	32.2 ± 2.2	144.4 ± 37.5	***	*	
FGF21 (pg·mL^{-1})	70.3 ± 14.5	75.9 ± 11.6	81.6 ± 11.7	90.1 ± 18.2			
TG (mmol L^{-1})	1.2 ± 0.2	0.8 ± 0.1	1.2 ± 0.3	0.7 ± 0.1	**		
FAs (μmol L^{-1})	380 ± 51	412 ± 22	270 ± 21	388 ± 39	*		
HDL-cholesterol (mmol L^{-1})	1.13 ± 0.08	1.17 ± 0.07	1.33 ± 0.11	1.44 ± 0.09			
LDL-cholesterol (mmol L^{-1})	3.20 ± 0.19	2.75 ± 0.15(^)	3.20 ± 0.19	3.59 ± 0.31			*
Total cholesterol (mmol L^{-1})	4.07 ± 0.17	3.58 ± 0.10^^	4.17 ± 0.14	4.60 ± 0.27			**
GIP (pmol L^{-1})	9.0 ± 1.1	15.2 ± 4.2	9.6 ± 1.7	8.9 ± 1.2			
GLP-1 (pmol L^{-1})	10.0 ± 1.1	15.3 ± 3.4	13.4 ± 2.2	13.3 ± 2.3			

Body composition and arterial plasma parameters obtained in the overnight-fasted state at pre intervention and after 6 weeks PUFA and SFA diet. Body composition parameters were determined using dual-energy X-ray absorptiometry (Lunar DPX-IQ dual energy X-ray absorptiometry scanner) after 4 hr of fasting. Data are means ± SE. Two-way RM ANOVAs were applied to test for effect of intervention and diet. (^)p = 0.064, ^^p < 0.01, ^^^p< 0.001 pre versus post. *p < 0.05, **p < 0.01, ***p < 0.001 main effect of intervention or diet group, or interaction between diet type and effect of intervention. ALAT, alanine aminotransferase; hsCRP, high-sensitivity C-reactive protein; FGF21, fibroblast growth factor 21; GIP, gastric inhibitory polypeptide; GLP-1, glucagon-like peptide 1; HDL, high-density lipoprotein; HOMA-IR, homeostatic model assessment of insulin resistance; LDL, low-density lipoprotein. n = 9 in all groups.

1976). Muscle content of the Rab GTPase-activating protein TBC1 domain family member 1 (TBC1D1) decreased after both interventions (Figure 1M). This diet-induced downregulation of TBC1D1 may have assisted in the substrate switching, as a role for TBC1D1 in regulation of FA oxidation was shown in TBC1D1-deficient mice (Dokas et al., 2013) and rats (Whitfield et al., 2017), and C2C12 muscle cells (Chadt et al., 2008). However, the precise role of TBC1D1 remains to be uncovered.

The protein content of AMP-activated protein kinase α2 (AMPKα2) increased after both interventions (Figure 1N), an adaptation likely beneficial to regulation of muscle energy homeostasis (Kjobsted et al., 2018). The intramyocellular TG (IMTG) content remained unchanged with both high-fat diets compared with pre intervention (Figure 1O). This could relate to the habitual sedentary activity level of the subjects, as previous studies have reported increased IMTG by 54%–57% in physically active men after one or 4 weeks' eucaloric intake of 54E%–60E% fat (Schrauwen-Hinderling et al., 2005; Kiens et al., 1987), and a remarkable ability in athletes to upregulate IMTG storage after just a few days of eucaloric high fat (60E%–69E%) intake (Jansson and Kaijser, 1982; Zderic et al., 2004). Thus, it appears that, in skeletal muscles of the present sedentary subjects, several molecular adaptations induced by diet contributed to an increased capacity for FA uptake and oxidation rather than storage.

Maintained Insulin Sensitivity and Metabolic Flexibility to Glucose

Despite a daily fat intake comprising ~240 g for 6 weeks, insulin-stimulated glucose uptake, measured directly at the level of skeletal muscle by the femoral a-v balance technique, revealed that peripheral insulin sensitivity was unchanged after both high-fat diets, consistent with the observations on the whole-body level (Figures 1A and 2A). This extends previous short-term interventions showing that whole-body insulin sensitivity remained unchanged after 2.5–3 weeks of eucaloric intake of 49E%–75E% fat (of mixed FA composition) in lean to overweight subjects (Borkman et al., 1991; Cutler et al., 1995; van Herpen et al., 2011), and reports of unchanged intravenous glucose tolerance after 1 week of PUFA, SFA, and monounsaturated FA replacement at 54E% total fat intake (Fasching et al., 1996).

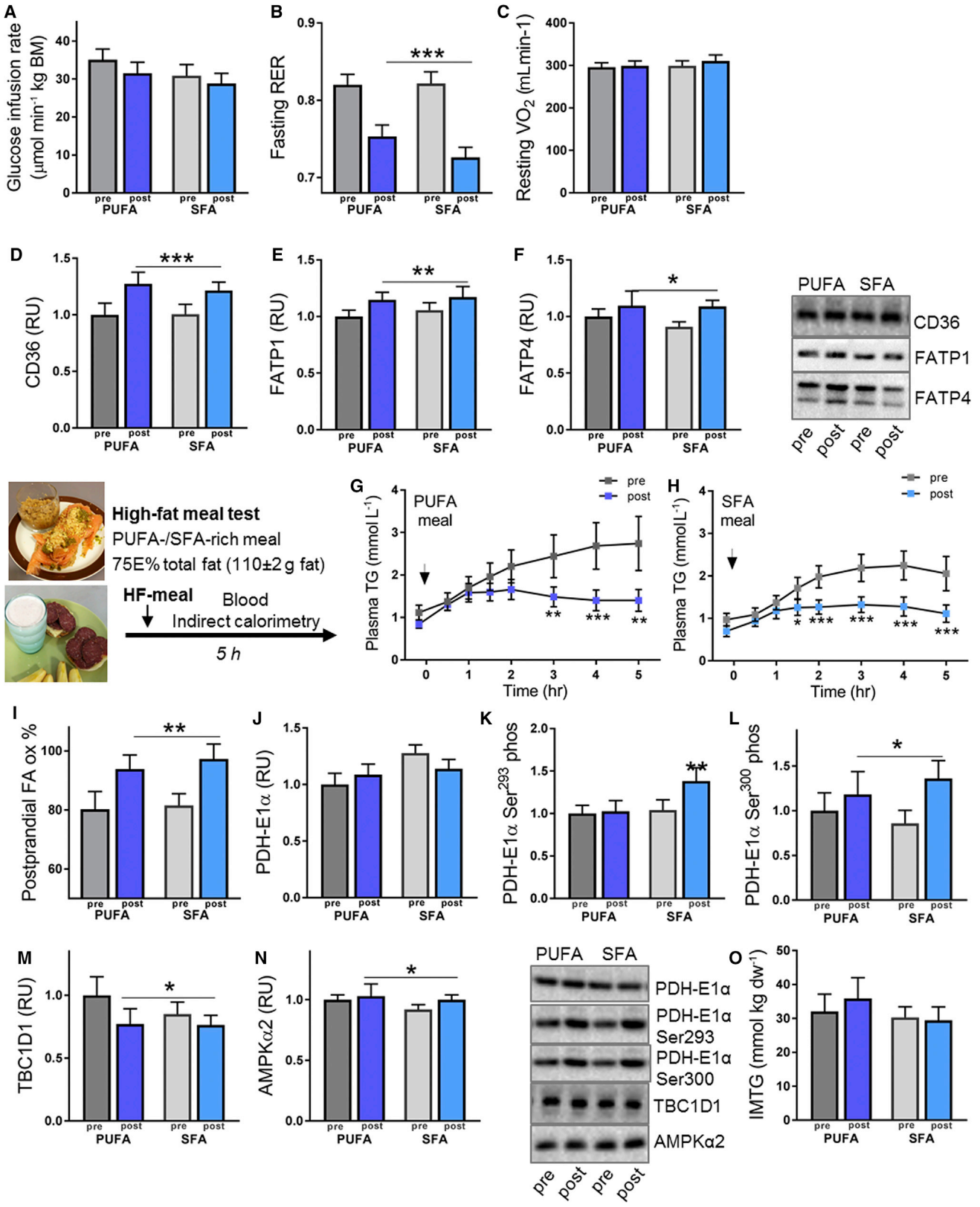

(legend on next page)

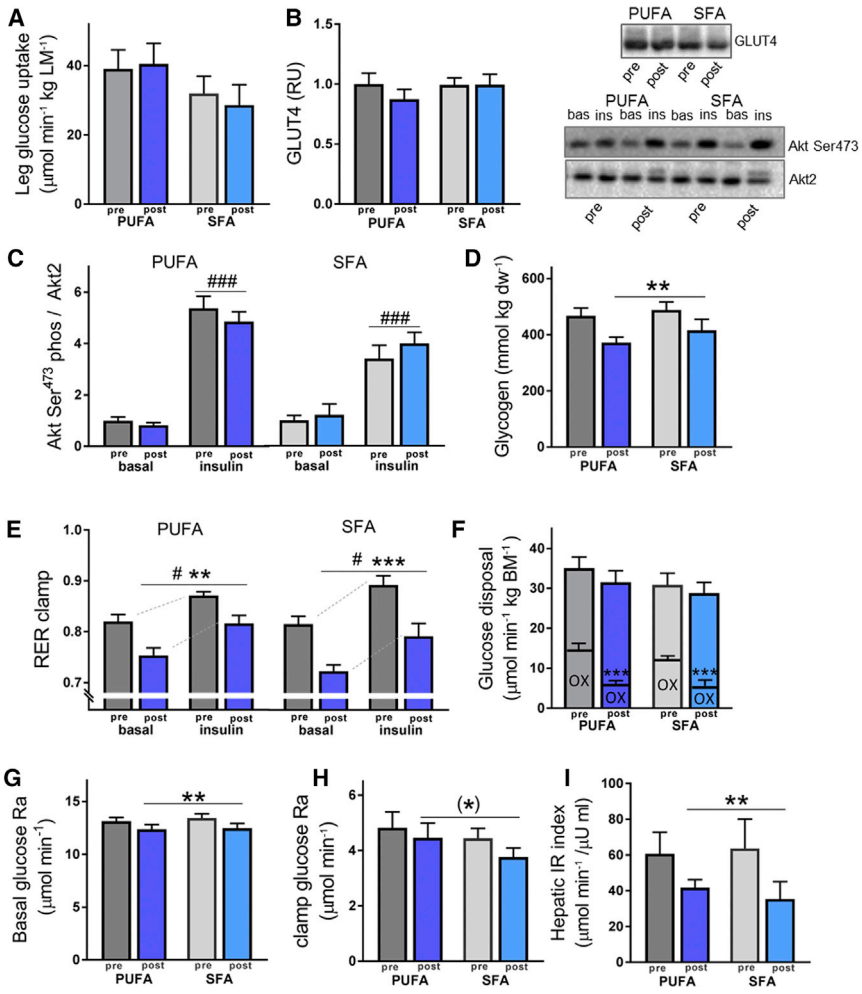

Figure 2. Peripheral Insulin Sensitivity, Expression, and Phosphorylation of Skeletal Muscle Proteins Involved in Glucose Metabolism and Hepatic Glucoregulation

(A) Insulin-stimulated leg glucose uptake, calculated as the arterialized femoral venous blood glucose difference multiplied by blood flow, and expressed per kilogram of leg mass (LM) as average values from the last 60 min of the clamp. No changes were obtained in the femoral arterial blood flow after the interventions.

(B and C) Muscle glucose transporter 4 (GLUT4) protein content and Akt Ser^{473} phosphorylation at basal and at end-clamp, expressed per Akt2 protein.

(D) Basal muscle glycogen content, expressed per kilogram dw.

(E) RER, obtained by indirect calorimetry in the basal state and at the end of the clamp.

(F) Oxidative glucose disposal (OX) calculated from indirect calorimetry during the last 60 min of the clamp, and illustrated with total glucose disposal.

(G) Basal hepatic glucose rate of appearance (Ra).

(H) Hepatic glucose Ra during the last 20 min of the clamp.

(I) Hepatic insulin resistance (IR) index.

Data are means ± SE. Western blot data are expressed as relative units, RU. Two-way RM ANOVAs were applied to test for effect of intervention and diet, or intervention and insulin. (*)$p = 0.096$, *$p < 0.05$, **$p < 0.01$, ***$p < 0.001$ effect of intervention. #$p < 0.05$, ###$p < 0.001$ effect of insulin. n = 9 in all groups.

The maintenance of glucose uptake in skeletal muscle in the present study was consistent with the observation that muscle GLUT4 protein content as well as basal and insulin-stimulated Akt Ser^{473} phosphorylation remained unchanged (Figures 2B and 2C). Hence, insulin signaling to glucose transport, as well as the capacity for glucose uptake, remained intact after the 6-week dietary intervention. The muscle glycogen content decreased in the resting, fasting state following both high-fat diets (Figure 2D). The marked induction of FA oxidation with both high-fat diets thus did not compromise insulin action. This is important and is furthermore supported by the maintained insulin-induced increase in RER during the clamp in both trials (Figure 2E), in keeping with the described relationship between metabolic flexibility and glucose disposal rate (Galgani et al., 2008). However, the basal non-insulin-stimulated RER values were markedly reduced after the high-fat interventions, and total oxidative glucose disposal during the clamp

Figure 1. Whole-Body Insulin Sensitivity, Fasting and Postprandial Substrate Metabolism, and Skeletal Muscle Expression of Proteins in Lipid Metabolism at Pre-intervention and after 6-Week PUFA and SFA Diet

(A) Glucose infusion rate during the hyperinsulinemic-euglycemic clamp, expressed per kilogram body mass (BM) as average values from the last 60 min of the clamp.

(B) Fasting respiratory exchange ratio, obtained by indirect calorimetry.

(C) Resting oxygen uptake (VO_2).

(D–F) Muscle protein content of CD36 (D), FATP1 (E), and FATP4 (F).

(G and H) Plasma TG concentration before and after intake of a high-fat meal, providing 60 kJ/kg body mass (5.4 ± 0.4 MJ). The meals were composed of 75E% fat, 14E% carbohydrate, and 11E% protein, and were enriched in PUFA (G) or SFA (H) in accordance with the respective intervention group.

(I) Postprandial FA oxidation, calculated as the cumulative percentage of FA oxidation during 5 hr after the meal, with indirect calorimetry applied every hour.

(J–N) Muscle pyruvate dehydrogenase E1α (PDH-E1α) protein (J), PDH-E1α Ser^{293} phosphorylation (K), PDH-E1α Ser^{300} phosphorylation (L), TBC1 domain family member 1 (TBC1D1) protein (M), and AMP-activated protein kinase α2 (AMPKα2) protein (N).

(O) IMTG content, expressed per kilogram dry weight (dw).

Data are means ± SE. Western blot data are expressed as relative units (RU). Two-way repeated measures (RM) ANOVAs were applied to test for effect of intervention and diet. *$p < 0.05$, **$p < 0.01$, ***$p < 0.001$ effect of intervention. n = 9 in all groups.

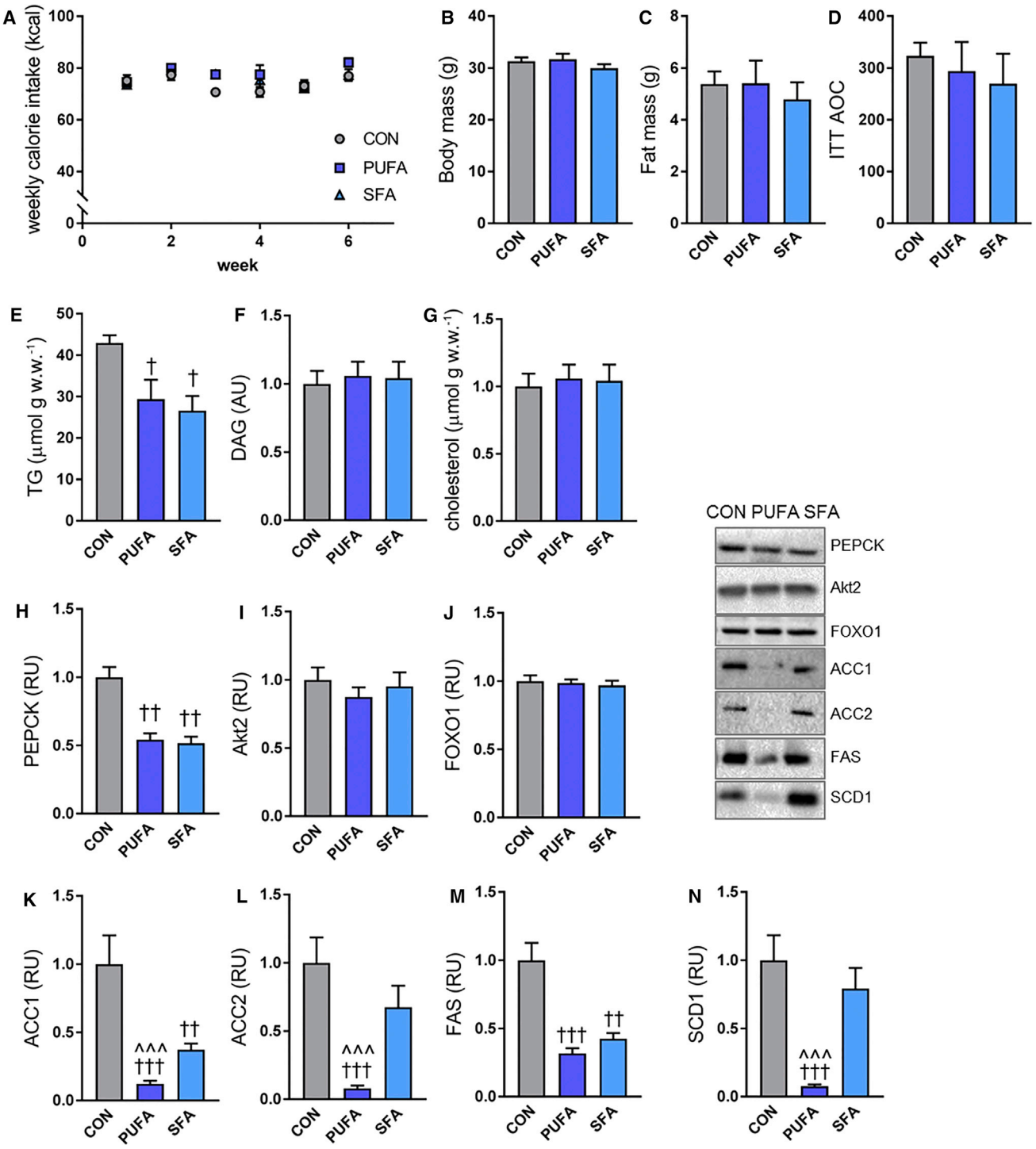

Figure 3. Calorie Intake, Body Composition, Insulin Sensitivity, and Hepatic Molecular Metabolism Obtained in Mice Fed Either the PUFA or SFA High-Fat Diet or a Low-Fat Reference Diet for 6 Weeks

(A) Weekly calorie intake, expressed as the weekly average per mouse. CON, control (reference diet).

(B) Body mass at week six.

(C) Fat mass, obtained from MRI scanning at the end of the intervention.

(D) Incremental area above the blood glucose curve (AOC) during an insulin tolerance test (ITT) (1 U/kg lean mass), calculated over 120 min.

(legend continued on next page)

was lower post intervention (Figure 2F), likely related to the moderate covalent inhibition of muscle PDH. Therefore, a larger fraction of the leg glucose uptake was directed toward non-oxidative glucose disposal, possibly facilitated by the lower muscle glycogen content.

Eucaloric High-Fat Diets Improve Hepatic Glucoregulation and Lipid Metabolism

The liver exerts a prominent role in regulation of systemic glucose as well as insulin levels. Hepatic glucose production was assessed by infusion of 6.6-$^{2}H_2$ glucose tracer for 2 hr before and during the clamp. Glucose production (Ra) was decreased in the fasting state after both the PUFA and SFA high-fat diet, and tended to be lower during the clamp, compared with pre intervention (Figures 2G and 2H). As the lower fasting glucose production was obtained concomitant with decreased fasting plasma insulin concentration (Table 1), the hepatic insulin resistance index was lowered post intervention (Figure 2I). Other dietary studies have also shown fasting glucose production to be decreased (Bisschop et al., 2001) or unchanged (Cutler et al., 1995; van Herpen et al., 2011; Chokkalingam et al., 2007) in healthy subjects after up to 3 weeks' intake of eucaloric diets with 41E%–83E% fat.

The hepatic insulin clearance, calculated from insulin and C-peptide concentrations before and during the clamp, increased after both high-fat diets (Table 1), reflected by the lower fasting plasma insulin concentration. Fasting plasma C-peptide concentration was not significantly changed. Together with the improved glucoregulation, the increased insulin clearance was indicative of hepatic insulin and glucose metabolism being altered in a beneficial and non-diabetic direction by eucaloric high fat and low carbohydrate intake. Of relevance to the present findings, we have also previously shown that 3 days' intake of a high-fat (79E%) and low-carbohydrate (10E%) diet increased insulin clearance compared with a control diet, despite 75% caloric excess (Lundsgaard et al., 2017b).

In our study, the fasting plasma TG concentrations were reduced after the PUFA (−33%) and SFA (−42%) high-fat interventions (Table 1). In contrast, plasma TG content increased >100% after 2 weeks of a eucaloric high-carbohydrate (75E%) diet, due to increased very-low-density lipoprotein (VLDL)-TG secretion (Mittendorfer and Sidossis, 2001). As fasting VLDL-TG secretion rate has been shown to be positively associated with hepatic TG content in healthy subjects (Fabbrini et al., 2008), the present findings may reflect lower hepatic TG accumulation after the diets. The assumption of lower hepatic TG content after the diets is also supported by our finding of increased hepatic insulin clearance after the diets since insulin clearance has been shown to be inversely related to hepatic TG content (Kotronen et al., 2007).

To evaluate possible diet-induced changes in *de novo* lipogenesis (DNL), plasma content of the FA marker C16:1n-7 palmitoleate was measured. This moiety represents the desaturated palmitate end product of DNL and its levels have been shown to correlate well with D_2O-measured DNL (Lee et al., 2015). The fasting plasma concentration of C16:1n-7 decreased after both high-fat diets, with a greater decrease after the PUFA (−62%) than after the SFA diet (−26%) (Table S3), indicative of decreased DNL. Presumably this represents an adaptive mechanism, protecting the liver from FA excess in the context of the increased dietary lipid load. A decreased DNL might be beneficial, considering the consistent observations of increased DNL in hepatic steatosis and liver insulin resistance (Sanders and Griffin, 2016). Furthermore, the plasma concentrations of the ketone body 3-hydroxybutyrate increased after both high-fat diets (Table 1) but were still markedly lower than levels of ~1 mM reported during prolonged exercise or 24 hr fasting (Puchalska and Crawford, 2017). This increased ketone production indicated an increased FA beta-oxidation in the liver; another adaptive mechanism to mitigate hepatic FA excess.

High-Fat Feeding Lowers TG Content and Capacity for Gluconeogenesis and DNL in Mouse Liver

To gain more insight into the beneficial effects of high fat and low carbohydrate intake on hepatic metabolism, two groups of C57BL/6J male mice were pair-fed the homogenized, freeze-dried, and pelleted human PUFA or SFA high-fat diets for 6 weeks, based on the caloric intake of a third group of mice on a starch-rich control diet with 7% fat. All mice were housed at 30°C thermoneutral conditions to better mimic human physiology (Ganeshan and Chawla, 2017). By feeding design, caloric intake was equal between all three groups, and body mass and fat mass were similar (Figures 3A–3C). An insulin tolerance test (1 U insulin/kg lean mass) revealed similar insulin-induced suppression of blood glucose (Figure 3D). Thus, similar to the human observations, insulin action was not impaired upon high-fat feeding without diet-induced obesity. This supports the notion that adverse effects of high-fat feeding in rodents might be more related to overfeeding than high fat intake per se. Thus, reduction in peripheral insulin sensitivity in rodents occurs with the onset of diet-induced increased adiposity (Turner et al., 2013; Kim et al., 2000).

After 6 weeks high-fat feeding, the hepatic TG content was 32% and 38% lower in PUFA- and SFA-fed mice, respectively, compared with control (Figure 3E). Liver contents of diacylglycerol (DAG) and total cholesterol were similar to control (Figures 3F and 3G). Molecular analyses at the protein level revealed that both high-fat diets led to a marked suppression of phosphoenolpyruvate carboxykinase (PEPCK), a key enzyme in gluconeogenesis, compared with the control diet (Figure 3H), congruent with the decreased glucose production in the human subjects. The protein contents of Akt2 and forkhead box O1 (FOXO1), involved in insulin action in the liver, were unchanged (Figures 3J and 3K).

One factor determining hepatic lipid accumulation is the rate of DNL relative to FA oxidation. Here, acetyl-CoA carboxylase

(E–N) Hepatic variables: (E) TG content, (F) DAG content, (G) total cholesterol content, (H) PEPCK protein, (I) Akt2 protein, (J) forkhead box protein O1 (FOXO1) protein, (K) acetyl-CoA carboxylase 1 (ACC1) protein, (L) ACC2 protein, (M) FAS protein, (N) stearoyl-CoA desaturase 1 (SCD1) protein. w.w., wet weight. Data are means ± SE. Western blot data are expressed as RU compared with CON. One-way ANOVAs were applied to test for differences between groups. $^{\dagger}p < 0.05$, $^{\dagger\dagger}p < 0.01$, $^{\dagger\dagger\dagger}p < 0.001$ compared with CON. $^{\wedge\wedge\wedge}p < 0.001$ compared with SFA. n = 9 mice in CON, n = 10 mice in the PUFA and SFA groups.

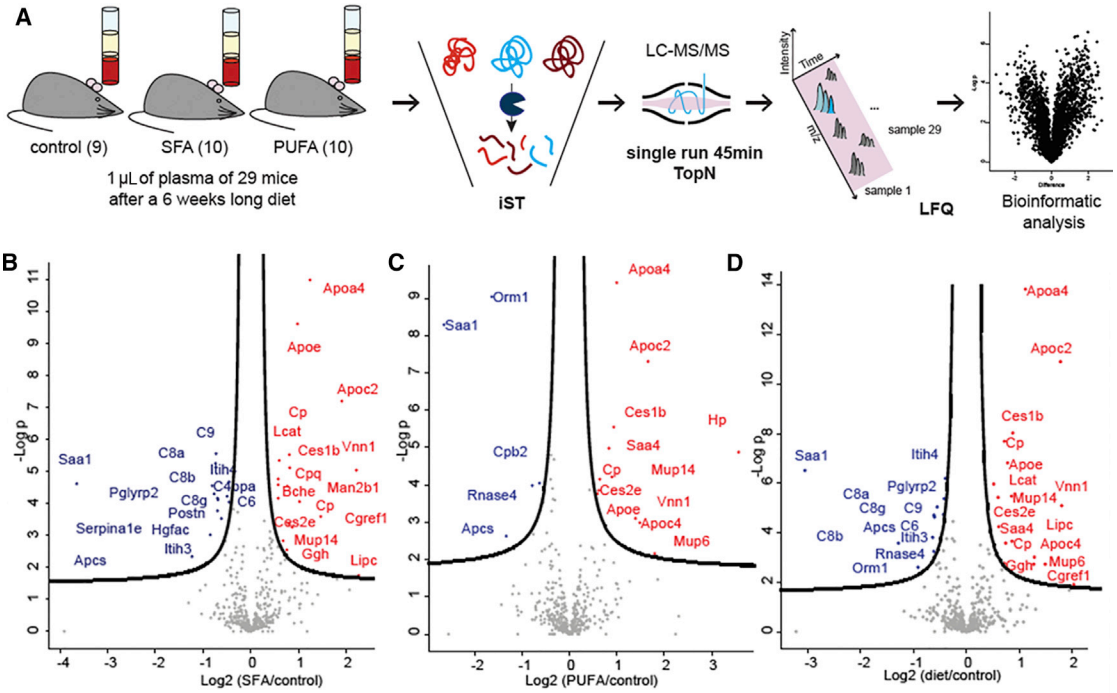

Figure 4. Plasma Proteomics of Mouse Plasma Obtained after 6 Weeks of High-Fat or Control Diet Feeding

(A) Proteomic workflow.

(B–D) Volcano plot of the plasma proteome after feeding with the PUFA high-fat diet (B), SFA high-fat diet (C), or both high-fat diets (D) compared with control, with the x axis depicting the fold change in protein levels expressed as log2 values and the y axis the log p value. p values were calculated based on a paired t test with s0 = 0.01 and 5% false discovery rate. iST, in-stage tip; LFQ, label-free quantification.

(ACC) is a key enzyme, regulating the production of malonyl-CoA, a substrate for DNL and an inhibitor of carnitine palmitoyl-transferase 1 (CPT1) and thereby mitochondrial FA entry. The indications of decreased DNL in the human study were confirmed in mouse liver, as ACC1 and FA synthase (FAS) protein were suppressed by both PUFA and SFA high-fat feeding, with additionally lowered ACC2 protein content in PUFA-fed mice compared with control (Figures 3K–3M). Gene suppression studies in rodent liver revealed that both ACC1 and ACC2 play a role in regulation of hepatic DNL and TG content (Mao et al., 2006; Harada et al., 2007; Savage et al., 2006). Expression of stearoyl-CoA desaturase 1 (SCD1), required for desaturation of the saturated DNL FA products, was markedly lower after PUFA compared with both control and SFA (Figure 3N). Together, these adaptations parallel the reduction of C16:1n-7 palmitoleate content in the human subjects, representing mechanisms to suppress DNL after high fat, and particular by PUFA, intake. The lipogenic gene suppression could result from inhibition of carbohydrate-responsive element-binding protein (ChREBP) nuclear translocation (Dentin et al., 2005) or inhibition of sterol regulatory element-binding protein 1 (SREBP1) activity (Takeuchi et al., 2010), as shown for PUFAs *in vitro*. These molecular findings nicely explain the beneficial effects of PUFAs, and particularly n-3 PUFAs, on nonalcoholic fatty liver disease revealed in clinical reports (Di Minno et al., 2012). Of note, the present observations in both human and mouse indicate that SFAs also have a suppressive effect on DNL.

High Fat Intake Changes the Plasma Proteome in Anti-inflammatory and Immune-Supporting Direction

To explore the quantitative changes in the plasma proteome in response to high fat intake at a global level, post-intervention mouse plasma and pre- and post-intervention human plasma were subjected to liquid chromatography-tandem mass spectrometry (LC-MS/MS)-based proteomics analysis (Figures 4A and S2). Lower variation in mouse compared with human plasma protein abundance was observed, with a greater variation for human plasma proteomics (Geyer et al., 2016) ascribed to technical challenges from the great dynamic protein range and high albumin abundance. Therefore, mouse proteomics data provided a more favorable basis for statistical interpretations.

The changes in protein abundance with the PUFA and SFA high-fat diets compared with the control diet or pre intervention for mouse and human plasma are depicted in Figures 4B and 4C and Figures S2A and S2B, respectively. In Figures 4D and S2C, plasma obtained post PUFA and post SFA was compared with control or pre intervention, to evaluate the effect of high-fat diet, independent of FA type. In mouse plasma, high fat intake per se increased plasma content of proteins related to lipoprotein metabolism and reverse cholesterol transport. Hence, the abundance of several proteins, as the apolipoproteins ApoC2 (3.5-fold) and ApoE (1.7-fold), Ces1b (1.8-fold), hepatic lipase (LipC) (1.7-fold), and LCAT (1.4-fold) were significantly upregulated (Figure 4D). In human plasma, abundance of CETP increased (1.3-fold), and ApoC3 decreased (−1.6-fold) with high-fat diet, independent of FA type (Figure S2C). Lowering of

ApoC3 would be indicative of increased lipid clearance, as ApoC3 inhibits hepatic lipase and lipoprotein lipase.

A decreased abundance in mouse plasma was observed for several proteins expressed in inflammation or immune responses after both high-fat diets; e.g., Saa1 (−8.3-fold), Orm1 (−1.9-fold), Itih4 (−1.3-fold), Pglyrp2 (−1.3-fold), and Apcs (−2.4-fold) (Figure 4D). This metabolic regulation in an anti-inflammatory direction was supported in human plasma by findings of reduced Saa4 (−1.1 fold) and the adipokine RBP4 after both high-fat diets (−1.1 fold) (Figure S2C). Adiponectin, an adipokine inversely associated with insulin resistance, increased after PUFA (1.3-fold) (Figure S2B).

Interestingly, the protein that exhibited the most significant change (i.e., increase) with both high-fat diets, and notably in plasma from both mouse (2.2-fold; Figure 4D) and human (1.4-fold; Figure S2C), was the apolipoprotein ApoA4. ApoA4 is primarily secreted from the small intestine and has recently been implicated in hepatic glucoregulation (Li et al., 2014). A regulatory role for ApoA4 in plasma TG clearance has been suggested, as individuals with an ApoA4 mutation have reduced postprandial plasma TG clearance (Hockey et al., 2001), and ApoA4 has been shown to increase the activity of plasma-derived lipoprotein lipase *in vitro* (Goldberg et al., 1990).

Incretin Hormones in Humans

The fasting plasma concentrations of the incretin hormones, gastric inhibitory polypeptide (GIP) and glucagon-like peptide 1 (GLP-1), were not changed after the high-fat diet intervention in humans (Table 1). Intake of a 75E% PUFA- or SFA-rich high-fat meal increased GIP and GLP-1 plasma levels postprandially with no differences between the PUFA and SFA meal, or pre- and post-intervention (Figure S3).

The Gut Microbiome Response to High Fat Intake in Humans and Mice

The human and mouse gut microbiomes were investigated before and after the interventions to examine whether alterations in community structures and/or functional potential could contribute to the uniform metabolic adaptations observed between species. In the human cohort, bacterial diversity was not affected by either time or diet (Figure S4A). In contrast, shifting from a purified low-fat diet to a complex human diet strongly boosted bacterial diversity in mouse fecal samples (Figure S4B), in agreement with the impact of diet complexity on gut microbial community structure (Dalby et al., 2017). However, in parallel with the human observations, the two groups of high-fat-fed mice did not differ in bacterial diversity (Figure S4B). At the level of operational taxonomic units (OTUs), the two high-fat diets distinctly affected gut microbiota composition in mice (ADONIS permanova, $p < 0.05$; Figure 5A) (DESeq on rarefied data [12,994 counts/sample], adjusted for individual and adjusted $p \leq 0.01$ as cutoff). In humans, the PUFA diet changed gut microbiome composition (ADONIS permanova, $p < 0.05$), whereas the SFA diet did not, despite SFA intake being elevated by 27E% (Figure 5A). Intake of the PUFA diet elicited an increase in the genera *Bacteroides* (log2FC: 1.66; $p = 0.005$) and *Lachnospira* (log2FC: 1.82; $p = 0.005$), and a decrease in *Bifidobacterium* (log2FC: −2.46; $p = 0.008$). Of note, *Bacteroides* has been implicated in attenuation of obesity and metabolic impairments (Ridaura et al., 2013). Interestingly, human and mice fed the same diet exhibited decreased similarity of the gut microbiome composition, where the distance between UniFrac-based centroids in the two host organisms increased after diet intervention (weighted UniFrac: SFA increased from 0.490 to 0.514, PUFA increased from 0.521 to 0.567; Figure 5A). However, as taxonomically different bacteria may support similar functional capabilities, we used PICRUSt to predict the functional potential of the microbiomes based on Kyoto Encyclopedia of Genes and Genomes (KEGGs). It is known that the human and mouse microbiomes share up to 95% of their functional potential, despite exhibiting less than 4% overlap at the gene level (Xiao et al., 2015). The high-fat diets, and especially the PUFA diet, led to a decreased distance between centroids of KEGG module abundances in humans and mice (Bray-Curtis dissimilarity: SFA decreased from 0.090 to 0.078, PUFA decreased from 0.104 to 0.057; Figure 5B) indicating similarities in the functional adaptation to the diets. Even though multiple KEGG modules showed organism-specific changes, 19 of the 23 modules affected by the PUFA diet in both humans and mice exhibited a similar pattern (Figure 5C). Thus, despite different microbiome taxonomical compositions, which is to be expected comparing mice and humans (Zhang et al., 2017), the functional capacity of the microbiome exhibited similar responses to the PUFA diet, with one of the most notable uniform changes being increased capacity for glycerol degradation. The modules that were altered in opposite direction between humans and mice most probably reflect differences between the human habitual diets and the less complex low-fat diet fed to the mice.

The Integrated Response of the Organism to High Fat Intake

Extensive metabolic adaptations enabled disposition of the fat without metabolic deterioration. Independent of dietary FA type, there was no induction of peripheral or hepatic insulin resistance in the healthy subjects, despite being overweight and inactive at baseline. In the present study, high fat and reduced carbohydrate provision induced anti-diabetic adaptations in hepatic glucoregulation and insulin clearance, as well as beneficial changes in fasting plasma TG concentration and DNL.

The fasting plasma concentration of fibroblast growth factor 21 (FGF21), which is mainly secreted by the liver (Hansen et al., 2015) and is proposed as a regulator of energy homeostasis (Fisher and Maratos-Flier, 2016), was unchanged with the high fat intake (Table 1). A similar lack of induction of circulating FGF21 levels was observed in a recent study of excessive high-fat overfeeding in healthy lean subjects (Lundsgaard et al., 2017a) and further suggests that high fat intake did not induce metabolic (i.e., mitochondrial and endoplasmic reticulum) stress in the liver, which in other settings has been linked to FGF21 induction (Salminen et al., 2017). The plasma concentration of the inflammatory marker high-sensitive C-reactive protein (hsCRP), an acute-phase protein of hepatic origin, tended ($p = 0.076$) to be decreased after both high-fat diets, with no changes in plasma alanine aminotransferase (ALAT) concentration (Table 1), a marker of liver health.

The PUFAs linoleic acid and α-linoleic acid are essentials for humans, and dietary provision is needed to ensure normal physiologic function. The PUFA diet was enriched in both n-6 and n-3

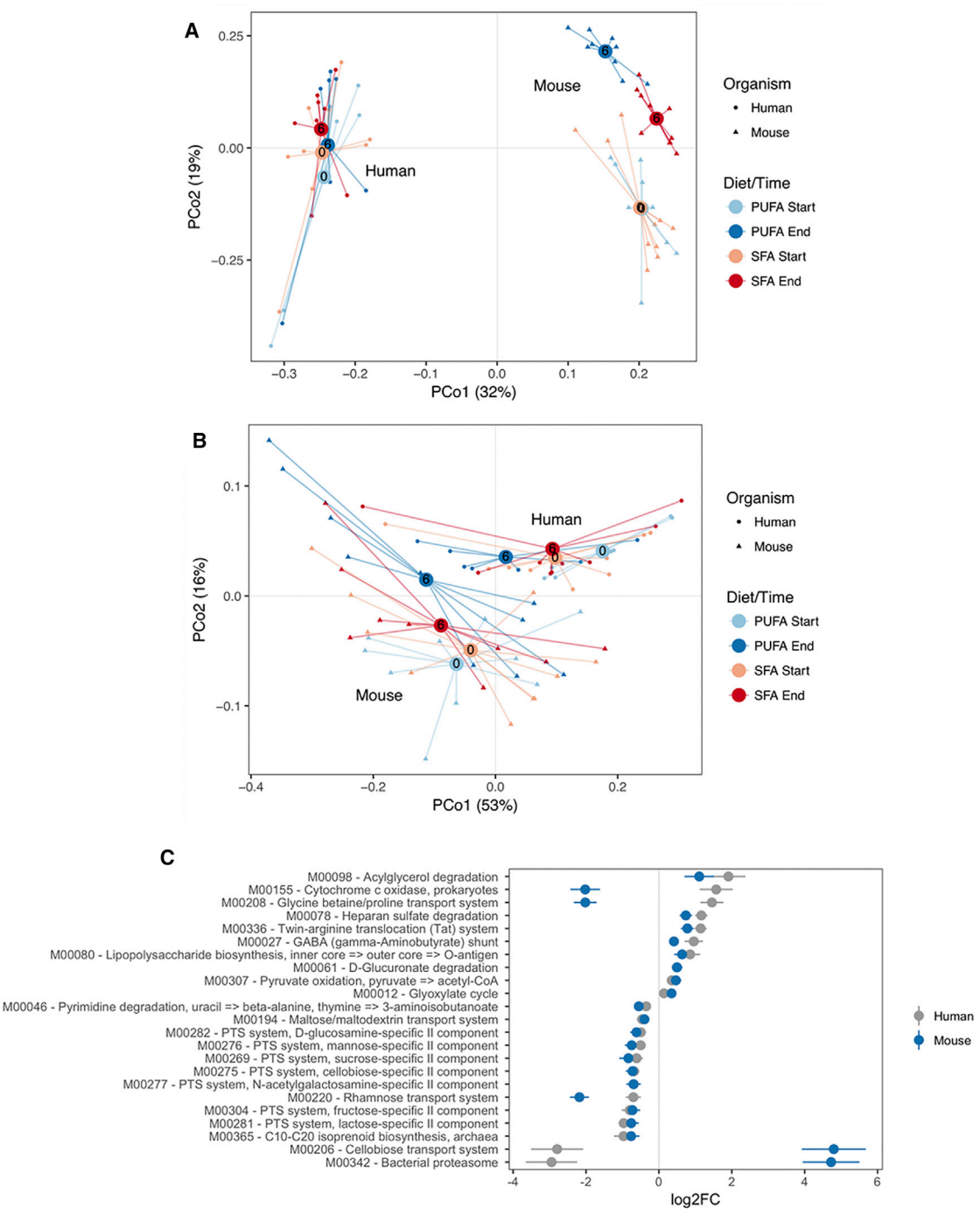

Figure 5. Microbiome Analysis of Human and Mouse Feces Obtained Before and after 6 Weeks of Diet Interventions

(A) Principal coordinate analysis (PCoA) plots using weighted UniFrac distances at OTU level.

(B) PCoA plot using Bray-Curtis dissimilarity index on KEGG module abundance. Large dots represent the centroids of the samples, which are represented by the smaller dots/triangles connected to the centroids. Week number is indicated in the centroids.

(C) Log2 fold change (start versus end) of the 23 KEGG modules significantly affected in both mice and humans on the PUFA diet, of which 19 modules show similar patterns in humans and mice on the PUFA diet. Error bars indicate SE.

PUFAs, and both experimental diets were designed to have an n-6/n-3 ratio close to 5.1 ± 0.8, characterizing the habitual diet (Table S1). Analysis of the FA composition of red blood cells (RBCs) (Table S4), reflecting long-term FA intake and metabolism, revealed that the PUFA diet increased RBC content of eicosapentaenoic acid and docosahexaenoic acid (DHA), and thus the omega-3 index to >8%, a level associated with low CVD risk (Harris et al., 2017). At the same time, RBC arachidonic

acid content was decreased (Table S4), likely as a result of Δ6 desaturase competition, suggesting that an n-6/n-3 ratio <5 could prove more beneficial when PUFA intake is high. The SFA in general induced fewer alterations in red cells but did lower RBC DHA content (Table S4).

The present study provides mechanistic insight explaining why a high fat intake, irrespective of FA saturation, is well tolerated when caloric balance is maintained. Overall, beneficial metabolic effects of high fat intake were observed for fasting insulin/glucose homeostasis and plasma TG levels, independent of FA type. Both high-fat diets induced similar increases in FA oxidation and molecular adaptations in skeletal muscle. Accordingly, the present study revealed that an increase in SFA intake by more than 200% was not associated with detrimental effects on metabolism or the evaluated health parameters. For some variables, PUFA intake was more potent to induce adaptations than SFA intake, as for the plasma cholesterol profile and suppression of DNL. Also, PUFA induced abundant changes in the composition and functional profile of gut microbiota.

Limitations of Study

The design of this carefully controlled intervention study, with numerous in-depth mechanistic analyses of molecular metabolism, limited the number of study participants, and future mechanistic studies are needed to explore whether the metabolic response to ingestion of high fat is influenced by gender, ethnicity, or age. Another relevant research question is whether obese individuals with metabolic impairments such as insulin resistance and/or dyslipidemia would adapt differently to high fat intake. The present subjects were chosen for being sedentary and overweight, representing a population group prone to develop metabolic disorders. A reduction of 12% in whole-body insulin sensitivity has been obtained with 4 weeks of eucaloric high fat intake in obese subjects (BMI 34 ± 1) (von Frankenberg et al., 2017). It is thus possible that a high dietary fat content may be less well tolerated in obese subjects with metabolic impairments rendering the switch to FA oxidation insufficient (Battaglia et al., 2012).

The study was designed with the aim of testing the response to a substantial dietary load of FAs. The FA availability was therefore by intention very high and not of a character likely to be implemented in daily living. Based on our study and previous shorter interventions, we speculate that extending the present dietary intervention for several months would be unlikely to alter the outcome significantly as long as the participants maintain a eucaloric diet and thereby avoid obesity.

The study was performed in men, and a similar study with female subjects would be of great translational value in subsequent studies. In more prolonged dietary intervention studies of pre-menopausal women, menstrual cycle phase and use of oral contraceptive must be considered. In a 1-week dietary intervention study, a 50E% high-fat diet actually increased whole-body insulin sensitivity by 10% in pre-menopausal, overweight women (Branis et al., 2015). Women may thus cope with a high fat content in the diet better compared with men, which could relate to their greater capacity for both muscle lipid storage and FA oxidation (Lundsgaard and Kiens, 2014).

The gut microbiome analyses were performed on fecal samples. Uptake of FAs occurs predominantly in the small intestine, and, hence, analysis of the fecal microbiome does not entirely reflect diet-induced compositional changes in the microbiome of the small intestine, which may affect uptake and impact on whole-body metabolism. It is likely that changes in the microbiome of the small intestine also play a role in the observed phenotypes. Sampling from the small intestine in humans is not trivial, and, accordingly, the vast majority of human microbiome studies have been limited to analyses of fecal samples. Still, compositional and functional analyses based on fecal samples have indeed proven relevant for multiple host phenotypes, including insulin action in humans and mice (Pedersen et al., 2016).

STAR★METHODS

Detailed methods are provided in the online version of this paper and include the following:

- KEY RESOURCES TABLE
- CONTACT FOR REAGENT AND RESOURCE SHARING
- EXPERIMENTAL MODEL AND SUBJECT DETAILS
  - Human Subjects
  - Mice
- METHOD DETAILS
  - Diets
  - Clamp Studies in Humans
  - High-Fat Meal Test in Humans
  - Mouse Experiments
  - Blood and Plasma Analyses in Humans
  - Human Skeletal Muscle Analyses
  - Mouse Liver Analyses
  - Microbiota Analysis in Humans and Mice
  - Plasma Proteome Analysis in Humans and Mice
- QUANTIFICATION AND STATISTICAL ANALYSIS
  - Calculations
  - Statistics
- DATA AND SOFTWARE AVAILABILITY

SUPPLEMENTAL INFORMATION

Supplemental Information includes four figures and six tables and can be found with this article online at https://doi.org/10.1016/j.cmet.2018.08.022.

ACKNOWLEDGMENTS

We acknowledge the skilled technical assistance of Irene Bech Nielsen and Betina Bolmgren (Dept. of Nutrition, Exercise and Sports, Copenhagen University). We also thank Astrid Elise Hasselberg at the Institute of Marine Research (IMR) for excellent assistance at the animal facility. The study was supported by the Danish Medical Research Council; the Lundbeck Research Foundation; the Max-Planck-Society for the Advancement of Science; the Novo Nordisk Foundation; and the University of Copenhagen Excellence Program for Interdisciplinary Research (2016), "Physical activity and Nutrition for Improvement of Health". K.A.S. was supported by a postdoctoral research grant from the Council for Independent Research/Medicine (grant number 4092-00309). The PhD scholarship of A.-M.L. was funded by the Danish Diabetes Academy, supported by the Novo Nordisk Foundation.

AUTHOR CONTRIBUTIONS

A.-M.L. and B.K. designed the study. A.-M.L., K.N.B.-M., K.A.S., T.S.N., J.R.H., S.L.H., J.F.P.W., E.A.R., and B.K. carried out the human experiments.

J.B.H., L.S.M., E.F., L.M., and K.K. designed and conducted the mouse study, with experimental contribution from K.A.S. A.-M.L., T.S.N., J.B.H., B.A.H.J., L.S.M., E.F., S.L.H., L.M., J.J.H., S.D., P.E.G., and A.S.D. contributed to the analyses. A.-M.L. and B.K. drafted the paper. All authors contributed to the final version of the manuscript.

DECLARATION OF INTERESTS

The authors declare no competing interests.

Received: March 2, 2018
Revised: June 21, 2018
Accepted: August 30, 2018
Published: September 27, 2018; corrected online: October 18, 2018

REFERENCES

Abubucker, S., Segata, N., Goll, J., Schubert, A.M., Izard, J., Cantarel, B.L., Rodriguez-Mueller, B., Zucker, J., Thiagarajan, M., Henrissat, B., et al. (2012). Metabolic reconstruction for metagenomic data and its application to the human microbiome. PLoS. Comput. Biol. *8*, e1002358.

Astrup, A. (2014). A changing view on saturated fatty acids and dairy: from enemy to friend. Am. J. Clin. Nutr. *100*, 1407–1408.

Aune, D., Norat, T., Romundstad, P., and Vatten, L.J. (2013). Dairy products and the risk of type 2 diabetes: a systematic review and dose-response meta-analysis of cohort studies. Am. J. Clin. Nutr. *98*, 1066–1083.

Battaglia, G.M., Zheng, D., Hickner, R.C., and Houmard, J.A. (2012). Effect of exercise training on metabolic flexibility in response to a high-fat diet in obese individuals. Am. J. Physiol. Endocrinol. Metab. *303*, E1440–E1445.

Bisschop, P.H., de Metz, J., Ackermans, M.T., Endert, E., Pijl, H., Kuipers, F., Meijer, A.J., Sauerwein, H.P., and Romijn, J.A. (2001). Dietary fat content alters insulin-mediated glucose metabolism in healthy men. Am. J. Clin. Nutr. *73*, 554–559.

Borkman, M., Campbell, L.V., Chisholm, D.J., and Storlien, L.H. (1991). Comparison of the effects on insulin sensitivity of high carbohydrate and high fat diets in normal subjects. J. Clin. Endocrinol. Metab. *72*, 432–437.

Borno, A., Foged, L., and van, H.G. (2014). Glucose and glycerol concentrations and their tracer enrichment measurements using liquid chromatography tandem mass spectrometry. J. Mass Spectrom. *49*, 980–988.

Branis, N.M., Etesami, M., Walker, R.W., Berk, E.S., and Albu, J.B. (2015). Effect of a 1-week, eucaloric, moderately high-fat diet on peripheral insulin sensitivity in healthy premenopausal women. BMJ Open Diabetes Res. Care *3*, e000100.

Caporaso, J.G., Kuczynski, J., Stombaugh, J., Bittinger, K., Bushman, F.D., Costello, E.K., Fierer, N., Pena, A.G., Goodrich, J.K., Gordon, J.I., et al. (2010). QIIME allows analysis of high-throughput community sequencing data. Nat. Methods *7*, 335–336.

Chadt, A., Leicht, K., Deshmukh, A., Jiang, L.Q., Scherneck, S., Bernhardt, U., Dreja, T., Vogel, H., Schmolz, K., Kluge, R., et al. (2008). Tbc1d1 mutation in lean mouse strain confers leanness and protects from diet-induced obesity. Nat. Genet. *40*, 1354–1359.

Chokkalingam, K., Jewell, K., Norton, L., Littlewood, J., van Loon, L.J., Mansell, P., Macdonald, I.A., and Tsintzas, K. (2007). High-fat/low-carbohydrate diet reduces insulin-stimulated carbohydrate oxidation but stimulates nonoxidative glucose disposal in humans: an important role for skeletal muscle pyruvate dehydrogenase kinase 4. J. Clin. Endocrinol. Metab. *92*, 284–292.

Cox, J., and Mann, M. (2008). MaxQuant enables high peptide identification rates, individualized p.p.b.-range mass accuracies and proteome-wide protein quantification. Nat. Biotechnol. *26*, 1367–1372.

Cutler, D.L., Gray, C.G., Park, S.W., Hickman, M.G., Bell, J.M., and Kolterman, O.G. (1995). Low-carbohydrate diet alters intracellular glucose metabolism but not overall glucose disposal in exercise-trained subjects. Metabolism *44*, 1264–1270.

Dalby, M.J., Ross, A.W., Walker, A.W., and Morgan, P.J. (2017). Dietary uncoupling of gut microbiota and energy harvesting from obesity and glucose tolerance in mice. Cell Rep. *21*, 1521–1533.

Dehghan, M., Mente, A., Zhang, X., Swaminathan, S., Li, W., Mohan, V., Iqbal, R., Kumar, R., Wentzel-Viljoen, E., Rosengren, A., et al. (2017). Associations of fats and carbohydrate intake with cardiovascular disease and mortality in 18 countries from five continents (PURE): a prospective cohort study. Lancet *390*, 2050–2062.

Dentin, R., Benhamed, F., Pegorier, J.P., Foufelle, F., Viollet, B., Vaulont, S., Girard, J., and Postic, C. (2005). Polyunsaturated fatty acids suppress glycolytic and lipogenic genes through the inhibition of ChREBP nuclear protein translocation. J. Clin. Invest. *115*, 2843–2854.

DeSantis, T.Z., Hugenholtz, P., Larsen, N., Rojas, M., Brodie, E.L., Keller, K., Huber, T., Dalevi, D., Hu, P., and Andersen, G.L. (2006). Greengenes, a chimera-checked 16S rRNA gene database and workbench compatible with ARB. Appl. Environ. Microbiol. *72*, 5069–5072.

Di Minno, M.N., Russolillo, A., Lupoli, R., Ambrosino, P., Di, M.A., and Tarantino, G. (2012). Omega-3 fatty acids for the treatment of non-alcoholic fatty liver disease. World J. Gastroenterol. *18*, 5839–5847.

Dokas, J., Chadt, A., Nolden, T., Himmelbauer, H., Zierath, J.R., Joost, H.G., and Al-Hasani, H. (2013). Conventional knockout of Tbc1d1 in mice impairs insulin- and AICAR-stimulated glucose uptake in skeletal muscle. Endocrinology *154*, 3502–3514.

Fabbrini, E., Mohammed, B.S., Magkos, F., Korenblat, K.M., Patterson, B.W., and Klein, S. (2008). Alterations in adipose tissue and hepatic lipid kinetics in obese men and women with nonalcoholic fatty liver disease. Gastroenterology *134*, 424–431.

FAO. (2010). Fats and fatty acid in human nutrition. Report of an expert consultation. http://www.who.int/nutrition/publications/nutrientrequirements/fatsandfattyacids_humannutrition/en/.

Fasching, P., Ratheiser, K., Schneeweiss, B., Rohac, M., Nowotny, P., and Waldhausl, W. (1996). No effect of short-term dietary supplementation of saturated and poly- and monounsaturated fatty acids on insulin secretion and sensitivity in healthy men. Ann. Nutr. Metab. *40*, 116–122.

Fisher, F.M., and Maratos-Flier, E. (2016). Understanding the physiology of FGF21. Annu. Rev. Physiol. *78*, 223–241.

Fritzen, A.M., Lundsgaard, A.M., Jordy, A.B., Poulsen, S.K., Stender, S., Pilegaard, H., Astrup, A., Larsen, T.M., Wojtaszewski, J.F., Richter, E.A., and Kiens, B. (2015). New Nordic diet-induced weight loss is accompanied by changes in metabolism and AMPK signaling in adipose tissue. J. Clin. Endocrinol. Metab. *100*, 3509–3519.

Galgani, J.E., Uauy, R.D., Aguirre, C.A., and Diaz, E.O. (2008). Effect of the dietary fat quality on insulin sensitivity. Br. J. Nutr. *100*, 471–479.

Ganeshan, K., and Chawla, A. (2017). Warming the mouse to model human diseases. Nat. Rev. Endocrinol. *13*, 458–465.

Geyer, P.E., Kulak, N.A., Pichler, G., Holdt, L.M., Teupser, D., and Mann, M. (2016). Plasma proteome profiling to assess human health and disease. Cell Syst. *2*, 185–195.

Goldberg, I.J., Scheraldi, C.A., Yacoub, L.K., Saxena, U., and Bisgaier, C.L. (1990). Lipoprotein ApoC-II activation of lipoprotein lipase. Modulation by apolipoprotein A-IV. J. Biol. Chem. *265*, 4266–4272.

Gormsen, L.C., Jessen, N., Gjedsted, J., Gjedde, S., Norrelund, H., Lund, S., Christiansen, J.S., Nielsen, S., Schmitz, O., and Moller, N. (2007). Dose-response effects of free fatty acids on glucose and lipid metabolism during somatostatin blockade of growth hormone and insulin in humans. J. Clin. Endocrinol. Metab. *92*, 1834–1842.

Hansen, J.S., Clemmesen, J.O., Secher, N.H., Hoene, M., Drescher, A., Weigert, C., Pedersen, B.K., and Plomgaard, P. (2015). Glucagon-to-insulin ratio is pivotal for splanchnic regulation of FGF-21 in humans. Mol. Metab. *4*, 551–560.

Harada, N., Oda, Z., Hara, Y., Fujinami, K., Okawa, M., Ohbuchi, K., Yonemoto, M., Ikeda, Y., Ohwaki, K., Aragane, K., et al. (2007). Hepatic de novo lipogenesis is present in liver-specific ACC1-deficient mice. Mol. Cell. Biol. *27*, 1881–1888.

Harris, W.S., Del, G.L., and Tintle, N.L. (2017). The Omega-3 Index and relative risk for coronary heart disease mortality: estimation from 10 cohort studies. Atherosclerosis *262*, 51–54.

Hockey, K.J., Anderson, R.A., Cook, V.R., Hantgan, R.R., and Weinberg, R.B. (2001). Effect of the apolipoprotein A-IV Q360H polymorphism on postprandial plasma triglyceride clearance. J. Lipid Res. *42*, 211–217.

Hoeg, L.D., Sjoberg, K.A., Jeppesen, J., Jensen, T.E., Frosig, C., Birk, J.B., Bisiani, B., Hiscock, N., Pilegaard, H., Wojtaszewski, J.F., et al. (2011). Lipid-induced insulin resistance affects women less than men and is not accompanied by inflammation or impaired proximal insulin signaling. Diabetes *60*, 64–73.

Holm, J.B., Sorobetea, D., Kiilerich, P., Ramayo-Caldas, Y., Estelle, J., Ma, T., Madsen, L., Kristiansen, K., and Svensson-Frej, M. (2015). Chronic *Trichuris muris* infection decreases diversity of the intestinal microbiota and concomitantly increases the abundance of lactobacilli. PLoS One *10*, e0125495.

Jansson, E., and Kaijser, L. (1982). Effect of diet on the utilization of blood-borne and intramuscular substrates during exercise in man. Acta Physiol. Scand. *115*, 19–30.

Kelstrup, C.D., Jersie-Christensen, R.R., Batth, T.S., Arrey, T.N., Kuehn, A., Kellmann, M., and Olsen, J.V. (2014). Rapid and deep proteomes by faster sequencing on a benchtop quadrupole ultra-high-field Orbitrap mass spectrometer. J. Proteome Res. *13*, 6187–6195.

Kerbey, A.L., Randle, P.J., Cooper, R.H., Whitehouse, S., Pask, H.T., and Denton, R.M. (1976). Regulation of pyruvate dehydrogenase in rat heart. Mechanism of regulation of proportions of dephosphorylated and phosphorylated enzyme by oxidation of fatty acids and ketone bodies and of effects of diabetes: role of coenzyme A, acetyl-coenzyme A and reduced and oxidized nicotinamide-adenine dinucleotide. Biochem. J. *154*, 327–348.

Kiens, B., Essen-Gustavsson, B., Gad, P., and Lithell, H. (1987). Lipoprotein lipase activity and intramuscular triglyceride stores after long-term high-fat and high-carbohydrate diets in physically trained men. Clin. Physiol. *7*, 1–9.

Kim, J.Y., Nolte, L.A., Hansen, P.A., Han, D.H., Ferguson, K., Thompson, P.A., and Holloszy, J.O. (2000). High-fat diet-induced muscle insulin resistance: relationship to visceral fat mass. Am. J. Physiol. Regul. Integr. Comp. Physiol. *279*, R2057–R2065.

Kjobsted, R., Hingst, J.R., Fentz, J., Foretz, M., Sanz, M.N., Pehmoller, C., Shum, M., Marette, A., Mounier, R., Treebak, J.T., et al. (2018). AMPK in skeletal muscle function and metabolism. FASEB J. *32*, 1741–1777.

Kotronen, A., Vehkavaara, S., Seppala-Lindroos, A., Bergholm, R., and Yki-Jarvinen, H. (2007). Effect of liver fat on insulin clearance. Am. J. Physiol. Endocrinol. Metab. *293*, E1709–E1715.

Krarup, T., and Holst, J.J. (1984). The heterogeneity of gastric inhibitory polypeptide in porcine and human gastrointestinal mucosa evaluated with five different antisera. Regul. Pept. *9*, 35–46.

Kulak, N.A., Pichler, G., Paron, I., Nagaraj, N., and Mann, M. (2014). Minimal, encapsulated proteomic-sample processing applied to copy-number estimation in eukaryotic cells. Nat. Methods *11*, 319–324.

Langille, M.G., Zaneveld, J., Caporaso, J.G., McDonald, D., Knights, D., Reyes, J.A., Clemente, J.C., Burkepile, D.E., Vega Thurber, R.L., Knight, R., et al. (2013). Predictive functional profiling of microbial communities using 16S rRNA marker gene sequences. Nat. Biotechnol. *31*, 814–821.

Lee, J.J., Lambert, J.E., Hovhannisyan, Y., Ramos-Roman, M.A., Trombold, J.R., Wagner, D.A., and Parks, E.J. (2015). Palmitoleic acid is elevated in fatty liver disease and reflects hepatic lipogenesis. Am. J. Clin. Nutr. *101*, 34–43.

Li, X., Xu, M., Wang, F., Kohan, A.B., Haas, M.K., Yang, Q., Lou, D., Obici, S., Davidson, W.S., and Tso, P. (2014). Apolipoprotein A-IV reduces hepatic gluconeogenesis through nuclear receptor NR1D1. J. Biol. Chem. *289*, 2396–2404.

Lie, O., and Lambertsen, G. (1991). Fatty acid composition of glycerophospholipids in seven tissues of cod (*Gadus morhua*), determined by combined high-performance liquid chromatography and gas chromatography. J. Chromatogr. *565*, 119–129.

Lowry, O.H., and Passonneau, J.V. (1972). A Flexible System of Enzymatic Analysis (Academic Press).

Lundsgaard, A.M., Fritzen, A.M., Sjoberg, K.A., Myrmel, L.S., Madsen, L., Wojtaszewski, J.F., Richter, E.A., and Kiens, B. (2017a). Circulating FGF21 in humans is potently induced by short term overfeeding of carbohydrates. Mol. Metab. *6*, 22–29.

Lundsgaard, A.M., and Kiens, B. (2014). Gender differences in skeletal muscle substrate metabolism - molecular mechanisms and insulin sensitivity. Front Endocrinol. (Lausanne) *5*, 195.

Lundsgaard, A.M., Sjoberg, K.A., Hoeg, L.D., Jeppesen, J., Jordy, A.B., Serup, A.K., Fritzen, A.M., Pilegaard, H., Myrmel, L.S., Madsen, L., et al. (2017b). Opposite regulation of insulin sensitivity by dietary lipid versus carbohydrate excess. Diabetes *66*, 2583–2595.

Mao, J., DeMayo, F.J., Li, H., Abu-Elheiga, L., Gu, Z., Shaikenov, T.E., Kordari, P., Chirala, S.S., Heird, W.C., and Wakil, S.J. (2006). Liver-specific deletion of acetyl-CoA carboxylase 1 reduces hepatic triglyceride accumulation without affecting glucose homeostasis. Proc. Natl. Acad. Sci. USA *103*, 8552–8557.

Mittendorfer, B., and Sidossis, L.S. (2001). Mechanism for the increase in plasma triacylglycerol concentrations after consumption of short-term, high-carbohydrate diets. Am. J. Clin. Nutr. *73*, 892–899.

Morio, B., Fardet, A., LeGrand, P., and Lecerf, J.M. (2016). Involvement of dietary saturated fats, from all sources or of dairy origin only, in insulin resistance and type 2 diabetes. Nutr. Rev. *74*, 33–47.

Orava, J., Nuutila, P., Noponen, T., Parkkola, R., Viljanen, T., Enerback, S., Rissanen, A., Pietilainen, K.H., and Virtanen, K.A. (2013). Blunted metabolic responses to cold and insulin stimulation in brown adipose tissue of obese humans. Obesity (Silver Spring) *21*, 2279–2287.

Pedersen, H.K., Gudmundsdottir, V., Nielsen, H.B., Hyotylainen, T., Nielsen, T., Jensen, B.A., Forslund, K., Hildebrand, F., Prifti, E., Falony, G., et al. (2016). Human gut microbes impact host serum metabolome and insulin sensitivity. Nature *535*, 376–381.

Pehmoller, C., Brandt, N., Birk, J.B., Hoeg, L.D., Sjoberg, K.A., Goodyear, L.J., Kiens, B., Richter, E.A., and Wojtaszewski, J.F. (2012). Exercise alleviates lipid-induced insulin resistance in human skeletal muscle-signaling interaction at the level of TBC1 domain family member 4. Diabetes *61*, 2743–2752.

Puchalska, P., and Crawford, P.A. (2017). Multi-dimensional roles of ketone bodies in fuel metabolism, signaling, and therapeutics. Cell Metab. *25*, 262–284.

Ridaura, V.K., Faith, J.J., Rey, F.E., Cheng, J., Duncan, A.E., Kau, A.L., Griffin, N.W., Lombard, V., Henrissat, B., Bain, J.R., et al. (2013). Gut microbiota from twins discordant for obesity modulate metabolism in mice. Science *341*, 1241214.

Salminen, A., Kaarniranta, K., and Kauppinen, A. (2017). Integrated stress response stimulates FGF21 expression: systemic enhancer of longevity. Cell Signal. *40*, 10–21.

Sanders, F.W., and Griffin, J.L. (2016). De novo lipogenesis in the liver in health and disease: more than just a shunting yard for glucose. Biol. Rev. Camb. Philos. Soc. *91*, 452–468.

Savage, D.B., Choi, C.S., Samuel, V.T., Liu, Z.X., Zhang, D., Wang, A., Zhang, X.M., Cline, G.W., Yu, X.X., Geisler, J.G., et al. (2006). Reversal of diet-induced hepatic steatosis and hepatic insulin resistance by antisense oligonucleotide inhibitors of acetyl-CoA carboxylases 1 and 2. J. Clin. Invest. *116*, 817–824.

Schrauwen-Hinderling, V.B., Kooi, M.E., Hesselink, M.K., Moonen-Kornips, E., Schaart, G., Mustard, K.J., Hardie, D.G., Saris, W.H., Nicolay, K., and Schrauwen, P. (2005). Intramyocellular lipid content and molecular adaptations in response to a 1-week high-fat diet. Obes. Res. *13*, 2088–2094.

Schwab, U., Lauritzen, L., Tholstrup, T., Haldorssoni, T., Riserus, U., Uusitupa, M., and Becker, W. (2014). Effect of the amount and type of dietary fat on cardiometabolic risk factors and risk of developing type 2 diabetes, cardiovascular diseases, and cancer: a systematic review. Food Nutr. Res. *58*, https://doi.org/10.3402/fnr.v58.25145.

Serup, A.K., Alsted, T.J., Jordy, A.B., Schjerling, P., Holm, C., and Kiens, B. (2016). Partial disruption of lipolysis increases postexercise insulin sensitivity in skeletal muscle despite accumulation of DAG. Diabetes *65*, 2932–2942.

Skovbro, M., Boushel, R., Hansen, C.N., Helge, J.W., and Dela, F. (2011). High-fat feeding inhibits exercise-induced increase in mitochondrial respiratory flux in skeletal muscle. J. Appl. Physiol. (1985) *110*, 1607–1614.

Steele, R. (1959). Influences of glucose loading and of injected insulin on hepatic glucose output. Ann. N. Y. Acad. Sci. *82*, 420–430.

Takeuchi, Y., Yahagi, N., Izumida, Y., Nishi, M., Kubota, M., Teraoka, Y., Yamamoto, T., Matsuzaka, T., Nakagawa, Y., Sekiya, M., et al. (2010). Polyunsaturated fatty acids selectively suppress sterol regulatory element-binding protein-1 through proteolytic processing and autoloop regulatory circuit. J. Biol. Chem. *285*, 11681–11691.

Turner, N., Kowalski, G.M., Leslie, S.J., Risis, S., Yang, C., Lee-Young, R.S., Babb, J.R., Meikle, P.J., Lancaster, G.I., Henstridge, D.C., et al. (2013). Distinct patterns of tissue-specific lipid accumulation during the induction of insulin resistance in mice by high-fat feeding. Diabetologia *56*, 1638–1648.

Tyanova, S., Temu, T., Sinitcyn, P., Carlson, A., Hein, M.Y., Geiger, T., Mann, M., and Cox, J. (2016). The Perseus computational platform for comprehensive analysis of (prote)omics data. Nat. Methods *13*, 731–740.

van Herpen, N.A., Schrauwen-Hinderling, V.B., Schaart, G., Mensink, R.P., and Schrauwen, P. (2011). Three weeks on a high-fat diet increases intrahepatic lipid accumulation and decreases metabolic flexibility in healthy overweight men. J. Clin. Endocrinol. Metab. *96*, E691–E695.

von Frankenberg, A.D., Marina, A., Song, X., Callahan, H.S., Kratz, M., and Utzschneider, K.M. (2017). A high-fat, high-saturated fat diet decreases insulin sensitivity without changing intra-abdominal fat in weight-stable overweight and obese adults. Eur. J. Nutr. *56*, 431–443.

Whitfield, J., Paglialunga, S., Smith, B.K., Miotto, P.M., Simnett, G., Robson, H.L., Jain, S.S., Herbst, E.A.F., Desjardins, E.M., Dyck, D.J., et al. (2017). Ablating TBC1D1 impairs contraction-induced sarcolemmal glucose transporter type 4 redistribution, but not insulin-mediated responses in rats. J. Biol. Chem. *292*, 16653–16664.

Xiao, L., Feng, Q., Liang, S., Sonne, S.B., Xia, Z., Qiu, X., Li, X., Long, H., Zhang, J., Zhang, D., et al. (2015). A catalog of the mouse gut metagenome. Nat. Biotechnol. *33*, 1103–1108.

Yost, T.J., Jensen, D.R., Haugen, B.R., and Eckel, R.H. (1998). Effect of dietary macronutrient composition on tissue-specific lipoprotein lipase activity and insulin action in normal-weight subjects. Am. J. Clin. Nutr. *68*, 296–302.

Zderic, T.W., Davidson, C.J., Schenk, S., Byerley, L.O., and Coyle, E.F. (2004). High-fat diet elevates resting intramuscular triglyceride concentration and whole body lipolysis during exercise. Am. J. Physiol. Endocrinol. Metab. *286*, E217–E225.

Zhang, L., Bahl, M.I., Roager, H.M., Fonvig, C.E., Hellgren, L.I., Frandsen, H.L., Pedersen, O., Holm, J.C., Hansen, T., and Licht, T.R. (2017). Environmental spread of microbes impacts the development of metabolic phenotypes in mice transplanted with microbial communities from humans. ISME J. *11*, 676–690.

STAR★METHODS

KEY RESOURCES TABLE

REAGENT OR RESOURCE	SOURCE	IDENTIFIER
Biological Samples		
Human skeletal muscle samples	This paper	N/A
Human blood samples	This paper	N/A
Human feces samples	This paper	N/A
Mouse liver samples	This paper	N/A
Mouse blood samples	This paper	N/A
Mouse feces samples	This paper	N/A
Chemicals, Peptides, and Recombinant Proteins		
6,6 $^2H_2$ glucose tracer	Cambridge Isotope Laboratories	DLM-349-PK
Human insulin	Novo Nordisk	Actrapid
Critical Commercial Assays		
Mouse control diet	Ssniff Specialdiäten	S8672-E050
Plasma insulin	ALPCO	80-INSHU-E01.1
Plasma c-peptide	ALPCO	80-CPTHU-E01.1
Plasma fatty acids	Trichem/Wako	NEFA C ACS ACOD 999-75406
Plasma triacylglycerol	Triolab	ABX PENTRA TG A11A01640
Plasma total-, HDL- and LDL-cholesterol	Triolab	A11A01636/A11A01638/A11A01634
Plasma 3-hydroxybutyrate	Randox	Ranbut kit
Microbial DNA	Macherey-Nagel	NucleoSpin Soil (740780)
Deposited Data		
Plasma proteomics data	ProteomeXchange Consortium via PRIDE	ProteomeXchange: PXD010516
Gut microbiota data	European Nucleotide Archive	ENA: PRJEB27768
Experimental Models: Organisms/Strains		
C57BL/6JBomTac male mice	Taconic	https://www.taconic.com/mouse-model/b6jbom
Software and Algorithms		
Prism 7	GraphPad	https://www.graphpad.com/scientific-software/prism/
SigmaPlot	Systat Software	https://systatsoftware.com/ products/sigmaplot/
R	The R Project for Statistical Computing	https://www.r-project.org/

CONTACT FOR REAGENT AND RESOURCE SHARING

Further information and requests for resources and reagents should be directed to and will be fulfilled by the Lead Contact, Bente Kiens (bkiens@nexs.ku.dk).

EXPERIMENTAL MODEL AND SUBJECT DETAILS

Human Subjects

18 healthy men with no family history of diabetes were recruited. Informed written consent was obtained, and the study was approved by the Copenhagen Ethics Committee (H-3-3012-129). The study was registered at https://clinicaltrials.gov/ (NCT03561363). The primary end-point variable of the study was whole-body insulin sensitivity. Subjects were assigned to the intervention groups by block randomization. The subjects in the PUFA and SFA groups were not different by age (32±6 and 33±6 yrs) (mean±SD), BMI (25.8±2.0 and 27.0±2.7 $kg \cdot m^{-2}$), body fat (26.2±4.7% and 28.4±5.0%) and physical activity level (VO_2peak 39±6 and 39±4 $ml \cdot kg^{-1} \cdot min^{-1}$).

Mice

Wildtype C57BL/6J BomTac male mice (Taconic, USA), eight weeks of age, were single-housed one week before initiating the diet interventions. All experiments followed the European convention for protection of vertebrate animals used for experiments and other scientific purposes. The animal experiment was approved by the Norwegian Animal Research Authority (Norwegian Food Safety Authority; FOTS id.nr 4878). Mice were kept at 30°C in 12 h light/dark cycle. The maintenance pre-intervention diet was a control diet with 7% (by weight) fat (S8672-E050, Ssniff Spezialdiäten, DE).

METHOD DETAILS

Diets

Habitual energy and macronutrient intake were evaluated from a three day weighed dietary registration and calculated (Dankost Pro, DK). Before the pre-intervention hyperinsulinemic clamp, subjects consumed a controlled eucaloric diet for three days with 54E% carbohydrate, 15E% protein and 29E% fat (Table S1), reflecting their habitual diet. The purpose of the short period of dietary control was to ensure that substrate metabolism was not acutely affected by abundant variations in food or energy intake in the days prior to pre-experimental testing, as well as to align muscle glycogen content, as variations here could introduce changes to peripheral insulin sensitivity. After the pre-intervention clamp, the high-fat diet interventions were initiated and continued until 11 P.M the evening before the post-intervention clamp. The main SFA sources were dairy products, fat-rich meat and palm oil, while the PUFA sources were vegetable oils (e.g. sunflower, linseed, grapeseed), salmon, nuts (e.g. walnuts, pecans, Brazil nuts) and grinded seeds (e.g. sesame and pine paste). The total protein intake was matched for the PUFA and SFA diets, and no major overall variation of the amino acid composition was observed between the experimental diets, and compared to the habitual intake (Table S5). Body weight maintenance was met by an energy intake of 14.1±0.3 and 14.0±0.3 MJ during the PUFA and SFA intervention, respectively.

Clamp Studies in Humans

On the clamp experimental day, the overnight fasted subjects arrived at 7.30 A.M., having abstained from vigorous physical activity for 48 hours. After 30 min at rest in the supine position, the resting respiratory exchange ratio (RER) was determined by indirect calorimetry. Catheters were inserted into an antecubital vein, a superficial dorsal hand vein, and the femoral vein in the groin. Arterialized blood samples from the dorsal hand vein (heated using a heating pad resulting in oxygen saturation in the blood between 93-95%) and samples from the femoral vein were obtained. Thereafter, a primed (priming dose 2.6 $mg \cdot kg^{-1}$), constant [6,6-$^2H_2$]-glucose tracer infusion (0.044 $mg \cdot kg^{-1} \cdot min^{-1}$) was carried out for 120 min, followed by a hyperinsulinemic-euglycemic clamp. During the clamp, glucose was infused from a 20% glucose solution enriched with 1.9% [6,6-$^2H_2$]-glucose. The clamp was initiated with an insulin bolus (9.0 $mU \cdot kg^{-1}$) (Actrapid, Novo Nordisk, DK) and continued for 120 min with an insulin infusion rate of 1 mU insulin $\cdot kg^{-1} \cdot min^{-1}$. The steady state plasma insulin concentrations were not different at pre- and post-intervention and averaged 94±7 and 84±5 μU/ml, and 91±8 and 90±5 μU/ml at pre- and post-intervention in PUFA and SFA, respectively. Plasma glucose was measured repeatedly and glucose infusion rate adjusted to match euglycemia, defined as the overnight-fasting arterial glucose concentration on the first experimental day. Every 20 min during the clamp, blood samples were simultaneously obtained from the femoral vein and the arterialized hand vein. Femoral arterial blood flow was determined by a laser ultra-sound Doppler technique (Philips iU22, ViCare Medical, DK). Indirect calorimetry was applied before, during and at the end of the clamp. Expired air was collected and analyzed, breath by breath, using an automatic gas-analysis system (Masterscreen CPX SB_X, CareFusion, Germany). Before and immediately at the end of the clamp, biopsies were obtained from the vastus lateralis muscle under local anesthesia from different incisions. The protocol was repeated after the diet interventions.

High-Fat Meal Test in Humans

Before the intervention and in week 6, the subjects in the PUFA and SFA group ingested a PUFA- or SFA-rich high-fat meal, respectively. The two high-fat meals contained 75E% fat, 14E% carbohydrate, 11E% protein and provided 60 kJ/kg body mass, corresponding to 5.4±0.4 MJ (Table S2). Subjects arrived after an overnight fast. After 45 min at rest, substrate oxidation was evaluated by indirect calorimetry, and a catheter inserted in the antecubital vein. After a basal blood sample, the high-fat meal was ingested over 10 min, together with 200 ml water. Postprandial venous blood samples were drawn at 30, 60, 90, 120, 180, 240 and 300 min, and indirect calorimetry applied every hour.

Mouse Experiments

The human PUFA and SFA diets were homogenized, freeze-dried and pelleted with a final energy content of 6.3 and 5.9 kcal/g, respectively. Nine mice were fed a Ssniff reference diet with 7% fat (mainly unsaturated), 53% starch, 11% sugar and 18% protein (S8672-E050, Ssniff, DE) (% by weight. Ten mice were fed the PUFA high-fat diet and ten mice the SFA high-fat diet, with energy provision adjusted to the caloric intake of mice fed the reference diet. Body composition was evaluated by MRI-scanning after week 4. At week 5, an insulin tolerance test was conducted in non-fasting mice. Insulin (Novo Nordisk, DK) was injected intraperitoneally (1 U/kg lean mass) and glucose was measured in blood from the tail vein before and 15, 30, 45, 60 and 90 min after the injection. At week 6 mice were anesthetized using isoflurane (Schering-Plow, DK) and sacrificed by cardiac puncture. Immediately thereafter the liver was collected and snap-frozen in liquid nitrogen.

Blood and Plasma Analyses in Humans

Glucose concentration was measured on an ABL615 (Radiometer Medical A/S, DK). Plasma insulin and C-peptide concentrations were measured by ELISA kits (ALPCO, USA). The concentration of FA (NEFA C kit, Wako Chemicals, DE), triacylglycerol (TG) (GPO-PAP kit, Roche Diagnostics, DE) and total-, HDL- and LDL-cholesterol (Roche Diagnostics, DE) in plasma were measured using colorimetric methods on an autoanalyzer (Hitachi 912, Boehringer, Germany). Plasma 3-hydroxybutyrate concentration was measured by a colorimetric method (Ranbut kit, Randox, UK) on a COBAS analyzer (Roche, DE). Plasma FGF21 concentration was measured by ELISA (FGF21 Quantikine ELISA kit, R&D Systems, USA). Plasma ALAT and high-sensitive CRP concentrations were measured by spectrophotometric and photometric methods (Vitros 5.1 FS, Ortho Clinical Diagnostics, USA). Plasma enrichment of the glucose isotope were measured using liquid chromatography mass spectrometry (ThermoQuest Finnegan AQA, USA) as described (Borno et al., 2014). For analyses of FA composition in plasma and red blood cells, lipids were extracted using chloroform/methanol, methylated using 12% BF_3 in methanol and separated and identified as described (Lie and Lambertsen, 1991). For analyses of GLP-1 and GIP, blood was treated with the DPP4 inhibitor valine-pyrrolidide (Novo Nordisk, DK) and the plasma concentrations of total GIP and GLP-1 were measured by RIA kits as described (Krarup and Holst, 1984).

Human Skeletal Muscle Analyses

Muscle samples were freeze-dried and dissected free of visible connective and adipose tissue under a microscope before analyses.

Muscle IMTG: Lipids were extracted in tetraethylammoniumhydroxid (E_4NOH) and proteins precipitated in perchloric acid. After centrifugation, the supernatant was neutralized in KHCO3 and glycerol units determined photometrically on a Pentra C400 analyser (Horiba, JA).

Muscle glycogen was determined fluorometrically as glycosyl units after acid hydrolysis (Lowry and Passonneau, 1972).

Western blot analyses: Tissue samples were homogenized in ice-cold lysis buffer as previously described (Fritzen et al., 2015). Lysate supernatants were collected after centrifugation for 20 min at 16.000 *g* at 4°C. For adipose tissue samples, the upper fat layer was carefully removed before lysates were collected. Protein concentrations were determined (Pierce Biotechnology, USA) and samples were heated (96°C) in Laemmli buffer before subjected to SDS-PAGE and semidry blotting. The primary antibodies are listed in Table S6. Immune complexes were visualized using Bio-Rad ChemiDoc MP Imaging System.

Mouse Liver Analyses

TG and cholesterol content: Liver tissue was homogenized 1 min in ice-cold extraction buffer (0.15 M natriumacetate in 25% Triton-X 100), heated for 3 min at 97°C and then centrifuged for 10 min at 9000 g. Supernatants were collected, and TG and cholesterol content measured photometrically on a Pentra C400 analyser (Horiba, JA).

DAG content was measured on freeze dried liver tissue by thin layer chromatography. Lipids were extracted in chloroform-methanol (2:1) and dissolved in chloroform, before being separated (Serup et al., 2016). Lipid staining were developed by a 10% copper sulfate pentahydrate and 8% phosphoric acid solution at 120°C for 15 min, and visualized and analyzed on a Kodak image station (Kodak 2000MM, DK). The DAG standard was from Sigma-Aldrich, USA.

Microbiota Analysis in Humans and Mice

Faecal samples from mice and humans were collected and frozen immediately. Bacterial DNA extraction (NucleoSpin soil kit, Macherey-Nagel), PCR-based library formation and sequencing (Illumina MiSeq) were performed as described previously (Holm et al., 2015). Raw sequencing data were processed using QIIME (Caporaso et al., 2010) including de novo-OTU picking, chimera-checking, and taxonomical assignment using the Greengenes database (DeSantis et al., 2006). Subsequent analyses were performed in R using Vegan, PhyloSeq and DESeq2. For PICRUSt (Langille et al., 2013) analysis, data were preprocessed using the pick_closed_reference_otus.py QIIME script against the Greengenes database. Using PICRUSt, the OTU table was normalized by 16S rRNA gene copy number and the functional metagenome was predicted using default settings. HUMAnN2 (Abubucker et al., 2012) was used to calculate the relative abundance of KEGG modules.

Plasma Proteome Analysis in Humans and Mice

Plasma samples were prepared according to the fast and highly reproducible workflow (Geyer et al., 2016) using an Agilent Bravo liquid handling platform. 1 μl plasma was added to 24 μl of the reducing and alkylating sodium deoxycholate buffer (Kulak et al., 2014) before protein denaturation at 100°C for 10 min. Proteins were then tryptic digested for four hours at 37°C and 1700 rpm. Peptides were acidified to a final concentration of 0.1% trifluoroacetic acid (TFA) for SDB-RPS binding and desalted before LC-MS/MS analysis. Samples were measured on a Q Exactive HF mass spectrometer (Kelstrup et al., 2014) coupled to an EASYnLC 1200 ultra-high-pressure system (Thermo Fisher Scientific, US) via a nano-electrospray ion source. About 1 μg of peptides were loaded on an in-house packed 40 cm HPLC-column (75 μm inner diameter; ReproSil-Pur C18-AQ 1.9 μm silica beads; Dr Maisch GmbH, Germany). Peptides were separated using a linear gradient from 3% B to 35% B in 37 min and stepped up to 75% in 4:30 min followed by a 3:30 min wash at 98% B at 450 nl/min where solvent A was 0.1% formic acid in water and solvent B was 80% acetonitrile, and 0.1% formic acid in water. Column temperature was kept at 60°C and the mass spectrometer was operated in 'top-15' data-dependent mode, collecting MS spectra in the orbitrap mass analyzer (60,000 resolution, 300-1,650 m/z range) with an automatic gain control (AGC) target of 3E6 and a maximum ion injection time of 20 ms. The most intense ions from the full scan were isolated with an isolation width of 1.4 m/z. MS/MS spectra were collected in the orbitrap (15,000 resolution) with an AGC target of 1E5 and a maximum

ion injection time of 25 ms. Precursor dynamic exclusion was enabled with a duration of 30 s. MS/MS spectra were searched against the mouse Uniprot database using MaxQuant (Cox and Mann, 2008) version 1.5.3.23. Label-free quantification of the mice and human plasma data was performed with the MaxLFQ algorithm using a minimum ratio count of 1. Data were interpreted using the Perseus software (Tyanova et al., 2016), version 1.5.5.0. We visualized the mean log2 ratios of biological replicates and the corresponding p-values with volcano plots and used t-test for binary comparison with s0=0.1 and a 5% FDR. For the human data, the proteins identified in the volcanoplots were the 15% with the lowest p-value and a log2 fold change $\geq$0.15 or $\leq$-0.15.

QUANTIFICATION AND STATISTICAL ANALYSIS

Calculations

Leg glucose uptake was calculated as the arterialized-femoral venous blood glucose concentration difference times the femoral arterial blood flow. Glucose rate of appearance (Ra) was calculated from the last 20 min of the basal and clamp period using steady-state equations (Steele, 1959). The hepatic IR index was calculated as glucose $Ra_{fasting}$ x [$insulin_{fasting}$], HOMA-IR index as ([$glucose_{fasting}$] x [$insulin_{fasting}$]) / 22.5, HOMA-β as 20 x [$insulin_{fasting}$]/[$glucose_{fasting}$] – 3.5 and basal hepatic insulin clearance as [$insulin_{fasting}$]/[C-$peptide_{fasting}$].

Statistics

All data are expressed as mean±SE, except subject characteristics (mean±SD). A Shapiro-Wilkinson test was performed to test for normal distribution. In few cases, where normal distribution was not obtained, this was achieved by log transforming data. The statistical parameters can be found in the figure legends. For variables dependent on time, a two-way RM ANOVA was performed to test for intervention and diet effects. Main effects and significant interactions were evaluated by Tukey post hoc testing. A one-way ANOVA was performed to test for differences between the groups of mice. A significance level of $p<0.05$ was chosen. Statistical analyses were performed in SigmaPlot (Systat Software, IL). For microbiota and plasma proteomics data in Figures 4 and 5, the statistics are described in the separate method sections.

DATA AND SOFTWARE AVAILABILITY

The accession number for the human and mouse mass spectrometry proteomics data reported in this paper is ProteomeXchange Consortium via the PRIDE repository: PXD010516. The accession number for the human and mouse microbiome data is European Nucleotide Archive: PRJEB27768.